Modification of ices by cosmic rays and solar wind

Hermann Rothard[1], Alicja Domaracka[1], Philippe Boduch[1], Maria Elisabetta Palumbo[2], Giovanni Strazzulla[2], Enio F. da Silveira[3], and Emmanuel Dartois[4]

[1]Centre de Recherche sur les Ions, les Matériaux et la Photonique,
Normandie Univ, ENSICAEN, UNICAEN, CEA, CNRS, CIMAP, 14000 Caen, France
[2]INAF–Osservatorio Astrofisico di Catania, Via S.Sofia 78, 95123 Catania, Italy
[3]Departamento de Física, Pontifícia Universidade Católica do Rio de Janeiro, Rua Marquês de São Vicente 225, 22451-900 Rio de Janeiro, RJ, Brazil
[4]Institut d'Astrophysique Spatiale, UMR8617, CNRS/Univ. Paris Sud, Université Paris Saclay, Univ. Paris Sud, F-91400 Orsay, France

E-mail : rothard@ganil.fr

Abstract

Astrophysical ices are exposed to different radiation fields including photons, electrons and ions. The latter stem from interstellar cosmic rays, the solar and stellar winds, shock waves or are trapped in the magnetospheres of giant planets. We briefly discuss the physics of energy deposition by radiation in condensed matter and experimental methods to study the induced effects. We then present results on radiation effects such as sputtering, amorphisation and compaction, dissociation of molecules, formation of new molecular species after radiolysis and by implantation of ions. The formation and radio-resistance of organic molecules, related to the question of the initial conditions for the emergence of life, are briefly discussed. This review is not meant to be comprehensive, but rather focusses on recent findings, with special emphasis on experiments with heavy multiply charged ion beams. These experiments aim in particular at simulating the effects of cosmic rays on icy grains in dense molecular clouds, and on the formation of molecules on icy bodies in the Solar System.

1. Introduction

Frozen gases that in astrophysics are collectively referred to as “ices” are ubiquitous in space. They are for instance present in the dense phases of the interstellar medium (ISM, e.g. dense molecular clouds, proto-stellar cores) and on numerous icy bodies in the Solar System. The molecules can be synthesized by surface reactions or freeze from the gas phase onto surfaces of dust grains, forming thin icy mantles if the temperatures are low; for example, temperatures in ISM can be as low as a few K. In the Solar System, ices form beyond a distance referred to as "frost line" or "snow line", actually located at 3-5 AU, and corresponding to temperatures of 150-170 K (Bennett, Pirim, Orlando 2013). These ices are continuously exposed to ionising irradiation (UV photons, electrons, ions); this may induce several physico-chemical processes. Among them are structural and phase changes, desorption and sputtering, fragmentation (radiolysis) subsequently followed by chemical reactions and possibly formation of new radicals/molecules.

In astrophysical studies on interaction of radiation with ices, effects induced by weakly ionising radiation (such as UV photons) and keV-MeV (mostly light) ions were extensively studied in the laboratory (Kanuchova *et al* 2016, Modica and Palumbo 2010, Garozzo *et a.* 2010, Moore, Hudson and Carlson 2007, Loeffler *et al* 2005, Carlson *et al* 2002, Cooper *et al* 2001, Gerakines *et al* 2000, Hudson and Moore 1999, Chrisey *et a*l 1990, Benit *et al.* 1988, *Johnson et al* 1987, Bar-Nun *et al* 1987, Brown *et al* 1987 to name some examples). This was driven by the use of keV to MeV ion accelerators, more common than swift heavy ion accelerators able to accelerate ions at much higher energies, which are large scale installations of which only a few exist in the world. Nowadays, also highly charged ion sources are available and can deliver slow beams with different charge states including completely stripped C, O and S. Although in space light ions (protons and helium) are often the dominant ones, here, we focus on the contribution of heavier ions (C, O, S, Fe), which are also present in space.

1.1 Where are ices, and what are they made of?

Boogert, Gerakines, and Whittet (2015) recently reviewed the infrared spectroscopic features of ices detected in space and discussed their abundances in space environments. Gas-grain chemistry taking place in the ISM, in dense cloud regions filled with gas and (sub-) micron sized refractory solid grains is an important factor for the increase in complexity of matter in the Galaxy. These clouds are the birthplace of protostellar objects, which progressively evolve from a large cloud of dust and eventually form a protoplanetary disk. Solid material exists in starless molecular clouds, recently born and thus still embedded stellar objects, protoplanetary disks, or in some mass loss envelopes (as results of ongoing chemistry). The observed so-called "ice mantles" are of specific interest amongst those solids, since they represent an interface between the refractory dust materials which formed the first grains, and the rich chemistry taking place in the gas phase.

Simple molecules such as H_2O, CO, CO_2, NH_3, CH_4, etc. are the dominant species, but more complex, organic molecules (alcohols etc.) have been detected. Considerably more molecules have been detected In the gas phase (http://astrochymist.org/astrochymist_mole.html) than in the solid phase, although it is thought that many of them are also present in the solid phase. This is due to the fact that radio-astronomical observations are able to detect the rotational bands of the molecules and are then order of magnitudes more sensitive than the IR astronomical observations necessary to observe the vibrational transitions of solid state molecules.

Since decades now, interstellar ices have been observed with ground based telescopes and several infrared space borne satellites (e.g. IRAS, ISO, Akari, Spitzer) towards many different lines of sight (the line between the observer and the source), pointing toward a large variety of astrophysical objects displaying ice features, see e.g. Neugebauer *et al* 1984, Kessler *et al* 1996, Werner *et al* 2004, Gibb *et al* 2004, Murakami *et al* 2007 and Öberg *et al* 2011. Some astrophysical objects are quite specific, like the circumstellar dust shells of evolved stars (e.g. so called OH-IR sources). Those oxygen rich post main sequence stars lose mass via stellar winds at a high rate, opaque to visible light and reemitting in the infrared. In these lines of sight, the ice mantles are likely to be dominated by H_2O, often the only ice present on dust grains, generally in crystalline form as it was formed in the gas phase high temperature chemistry taking place there, and then condensed at temperatures high enough for the ice to be crystalline.

More widely distributed in galaxies, large amounts of ice mantles are observed inside dense molecular clouds formed by surface reactions and/or gas condensation, and in objects resulting from their evolution (protostars and circumstellar disks). Observing ices signatures, most dominant in the near to mid infrared spectral region, requires an infrared background source to probe absorption. Among these probes, field stars located behind molecular clouds, allow the observers to use their infrared pencil beam to probe the foreground ice composition. They are crucial to understand ice evolution and chemistry in quiescent molecular clouds. The drawbacks are that they are statistically scarce and quite faint in the infrared. Also, being typically lower photospheric temperature main sequence stars, they often possess intrinsic photospheric molecular absorptions which have to be correctly removed to interpret the data.

Embedded protostellar objects and circumstellar disks constitute by far the more abundant and richest database of ice species. The drawback of these sources lines of sight is that the central object has sometimes started to interact radiatively with the ice-containing parental cloud, stimulating new energetic processes toward molecular complexity, but also complicating the analysis. In some cases, ices are also possibly observed in absorption/emission in the far-infrared in these objects (Maldoni *et al* 2003, Molinari *et al* 1999, Dartois *et al* 1998, Omont *et al* 1990). These numerous lines of sight, to which must be added the ones that to date escape detection such as optically thick disks, suggest that ices are very common and abundant constituents in the lifecycle of dust in galaxies.

The Solar System results from the evolution of one of such disks, which resulted in the formation of giant icy planets and also of smaller icy bodies and comet reservoirs. In the Kuiper belt and the Oort cloud of the Solar System, icy bodies containing also dust (carbon based materials, silicates), some of them being the progenitors of comets are present because of the dynamical planetary evolution. In those regions of the outer Solar System, frozen molecules can cover the surfaces of Trans Neptunian Objects (TNOs). The latter comprise Kuiper Belt objects (KBOs) including also dwarf planets like Pluto, Scattered disk objects (SDOs) with eccentric orbits at 30-100 AU (influenced by Neptune), and Oort Cloud objects (OCOs) at 2000-50000 AU. It is impressing that the estimated number of large icy KBOs (> 1 km) is about 10^6, and an even larger (of the order of 10^8) for OCOs (Bennett, Pirim and Orlando 2013). Ice thick layers, in most cases dominated by water molecules with few exceptions (Io, Titan) are also present on the giant planet's (Jupiter, Saturn) major satellites.

1.2 The complex radiation field in space

The icy bodies in space are exposed to a complex radiation field, where different kinds of radiation are acting simultaneously. Concentrating on ionising radiation, we can say that photons in a wide range of energy (UV, x-rays, gamma rays), electrons and positively charged particles (protons, helium, heavy ions of different charge state) contribute to the processing of ice layers in space and participate efficiently to their destruction, but also to evolution toward more complex molecules.

In particular, UV and cosmic ray irradiation play an important role in physical and chemical modifications of solids at low temperatures. The standard UV radiation field, resulting from the mean emitted spectrum of the expected distribution of different stars in the Galaxy, yields about 10^7-10^8 photons cm^{-2} s^{-1} in the 6 to 13.6 eV (hydrogen ionisation threshold) range (e.g. Draine 1978). A detailed discussion about fluxes was recently provided by Bennett, Pirim and Orlando (2013), see also references therein. In the denser and external UV shielded regions, the UV photons flux is generated by electronic transitions of H_2 after excitation by electrons produced by cosmic rays (Gredel et al. 1989).

1.3 Ions: cosmic rays, solar wind, magnetospheres

The Galaxy is immersed in a high-energy cosmic ray (CR) particle field. The CR energies extend from ~keV up to 10^{21} eV, and the lower part of the CR differential flux distribution has the highest impact on the modification of ices. From the energy distribution of CRs and the CR stopping power in typical interstellar dust grains, it can be estimated that the typical weighted energy for the interaction will be peaking around ~100 MeV/u, whereas in the high energy plasma it will reach a fraction of MeV/u. The enrgy of particles in stellar winds will be in the keV/u range (e.g.: Bringa and Johnson 2003). Within circumstellar disks, protostellar objects and dense clouds, the distribution of energies of ions is dependent on the position within the object and the expected CR distribution propagated and

impinging on the cloud (Padovani *et al* 2013, Chabot 2016). In evolved objects such as the Solar System, the central star also participates to the ion budget, the planets magnetic fields modify locally the ion energies and trajectories, and the irradiation dose varies locally and with the heliocentric distance.

Close to the Sun the main source of ions is the solar wind, then come ions accelerated by the solar and interplanetary shocks, and in the outer part higher energy ions from Galactic cosmic rays travelling in the local ISM (e.g. Cooper *et al* 2003). The energy distribution of theses ions can be very broad, but typical energies implied vary from the keV/u range for stellar winds, whereas magnetospheric ions will go up to the MeV/u, and Galactic cosmic rays in the 100MeV/u-GeV/u (Bringa *et al* 2003). Interaction with ions trapped in magnetospheres in the Solar System will be most important for icy bodies evolving around the giant planets Jupiter and Saturn, which possess magnetic fields of up to an order of magnitude stronger that of the Earth, and extending to much larger distances. In the Jupiter system, many of the moons can be exposed to highly energetic particles (tens of keV up to 100 MeV), inducing radiolysis and reactions with implanted ions (see e.g.: Cooper *et al* 2001). Uranus and Neptune have strongly tilted magnetospheres of medium size in between those of Earth and Jupiter.

1.4 Physics of interaction and energy transfer

The effects occurring when energetic particles interact with condensed matter result from transfer of energy and momentum, leading also to a decrease of velocity and kinetic energy of the projectile. Radiation physics therefore deals with two classes of phenomena: (1) the fate of the projectile after interaction with matter (slowing down, scattering and energy loss, projectile fragmentation, charge exchange etc.) and (2) the fate of matter. Starting point for understanding the class (2) phenomena are "elastic" and "inelastic" projectile-target atom collisions. In elastic collision with target atoms, the ion transfers a part of its momentum to the target nuclei. This may lead to a cascade of recoiling target atoms and possibly sputtering of target atoms from the surface. This process is usually referred to as "nuclear stopping" (S_n) and characterized by a microscopic friction force called nuclear stopping power, S_n.

The target electrons can be scattered by the projectile's (screened) Coulomb potential and the atom can be ionised (or excited) during such inelastic collisions ("electronic stopping", S_e). This may lead to the ejection of secondary electrons and photons (e.g. X-rays). In condensed matter, electrons from primary ionisation travel through the medium and may suffer elastic scattering by target atoms, or inelastic scattering by target electrons (referred to as electron transport). The latter inelastic processes may lead to further ionisation and creation of secondary, tertiary etc. electrons (cascade multiplication). Often, the fast primary electrons are called "delta-rays", and their range determines the maximum track diameter ("ultra-track"). The zone of high ionisation density close to the ion trajectory is sometimes called "infratrack" or "track core". There is, of course, a continuous evolution of the

radial (R) distribution of deposited energy around the ion track. It follows essentially a R^n dependence with $n \approx -2$ (Spohr 1990). This all happens within about 10^{-14} seconds and is usually referred to as "physical stage" during which the ionisation track develops. For a review of swift ion induced ionisation and electron transport related to energy deposition in condensed matter see Rothard and Gervais (2006).

The energy loss (and the nuclear and electronic contributions) per unit path length ($S_{total} = S_n + S_e$) is shown as a function of projectile energy for different ionic projectiles relevant to astrophysical environments in Figure 1. The energy loss in the high energy regime can easily be estimated from the transfer of energy or momentum in binary ion-electron collisions, i.e. scattering of an electron in the projectile's electrical Coulomb field (Bohr 1948, Sigmund 2006, 2014 and Jackson 1975). Other approaches are dielectric theory, i.e. the macroscopic description using a dielectric function $\varepsilon(\omega,\underline{\boldsymbol{k}})$ which parametrizes the dielectric responses (polarization) of the medium (Lindhard 1963, Jackson 1975, Etchenique, Flores and Ritchie 1990), and quantum mechanical perturbation theory (Bethe 1930,1933 and Bloch 1933a,b).

The essential result common to all of these approaches is a $S_e \sim n_e Z_p^2/v_p^2$ dependence in the perturbative regime, when the target electron velocity, v_e, is small is small compared to the projectile velocity, $v_p >> v_e$, and if the projectile is completely stripped. The electronic stopping is proportional to the square of the projectile charge (this reflects the scattering in the Coulomb potential) and decreases with the square of the projectile velocity. Furthermore, it is proportional to the number of target electrons encountered by the projectile. Most often in the literature, the so-called Bethe-Bloch formula is quoted, either in a relativistic form or in the non-relativistic limit. Note that for relativistic projectile velocity, the electronic energy loss is essentially constant.

At medium energy, around the maximum value of the energy loss, charge exchange (Betz 1972) comes into play. The complicated processes include electron capture, electron loss and formation and transport of excited projectile states versus de-excitation (radiative, Auger electron emission) through the medium. An ion with a given incoming charge state q_i can capture or (if $q_i < Z_p$) lose electrons. The actual charge and excitation state is penetration depth dependent with a dynamical evolution until equilibrium is reached (Betz 1972, Sigmund 2014). After a sufficient number of collisions, in other words, at a certain thickness, the equilibrium charge state distribution (independent of the initial charge q_i) is reached. We note that the energy loss associated to a given charge state can be calculated with the CasP code by Schiwietz and Grande (2011). In this regime, around the maximum stopping power, it is convenient to introduce a so-called effective charge $Z^*(v_p) = Z_p\,(1 - \exp[-(Z_p^{-2/3}\, v_p/v_0)]$ instead of Z_p; here, v_0 is the atomic unit of velocity referred to as "Bohr velocity" (Spohr 1990, Ziegler, Biersack and Ziegler 2008, Sigmund 2014). Electron loss is like a binary encounter collision between target nucleus and projectile electron, and therefore only relatively weekly dependent on projectile velocity. In contrast, electron capture depends on the velocity matching of projectile and target electrons (the overlap of their Compton profiles), and therefore strongly decreases

with projectile velocity so that electron loss dominates at low energy. This explains the velocity dependence of the effective charge.

Below the maximum stopping power, quasi-molecules are formed since v_p is lower than the target electron orbital velocity, $v_p << v_e$, referred to as LSS-Firsov regime (Firsov 1959, Lindhard, Scharff, Schiøtt 1963). The stopping is linear in the projectile velocity v_p and this closely resembles a friction phenomenon. All of these regimes belong to the electronic stopping S_e and contribute to material modification via deposition of the projectile kinetic energy on target electrons.

At very low velocities, with highly charged ions, other electronic processes linked to the potential energy of the projectile may occur: close to the surface, the potential energy of the projectiles can contribute to energy deposition via the capture of target electrons. At low velocities, nuclear stopping S_n is dominant and may lead to recoils and collision cascades. The nuclear stopping power as a function of projectile energy can be parametrized by empirical formulae as widely used in numerical simulations such as SRIM (Ziegler, Biersack, Ziegler 2008). For a detailed discussion on energy loss and charge changing phenomena, see Betz (1972), Sigmund (2006, 2014).

1.5 Differences and similarities with electrons and photons (UV, x-rays)

UV and cosmic rays (in the electronic interaction regime) share characteristics but also display differences in the interaction with interstellar ice mantles. Both irradiations are able to break bonds and ionise species, form radicals that further evolve in the ice. Main differences are found in the penetration depth in the mantles, determined by electronic transitions in the UV case, and thus sensitive to the optical constants of the ice mixtures, whereas for ions the energy and stopping power of the mixture dominate (e.g. Spinks and Woods 1990, Gerakines 2001). In addition, UV photons do not generally propagate to large distances when their energy lies above the ionisation threshold of hydrogen, the major constituent in space. Therefore ions are able to interact with ice species that remain otherwise mostly unaffected by direct electronic excitation from photons below the hydrogen ionisation threshold (e.g. N_2).

Nevertheless, experiments with realistic interstellar ices analogues show that, to first order, within the context of complex ice mixtures, the same kind of chemical species are globally observed with ions and UV photons irradiations if the same effective doses are applied, even if the newly formed species cross sections are different (e.g. Gerakines *et al* 2001, Baratta *et al* 2002, Munoz-Caro *et al* 2014, Islam *et al* 2014) and evolve with the dose, due to the change in optical properties affecting the UV penetration, and the relative amount of species.

2. Experimental aspects

Laboratory simulations on effects induced by ionising radiation on astrophysical ices, first of all, require one (or several) radiation sources. Widely used are UV lamps which are small and readily available. Higher energy photons, x-rays, can be delivered by relatively small electron bombardment

sources (as used for x-ray diffraction analysis or radiography) or the now worldwide widely available electron synchrotron light sources. Commercially available electron guns cover a wide range of energies from 0 to some hundred keV. Well known to the "atomic and molecular collisions" community are low energy ion sources and ion accelerators (see 2.1).

Second, a dedicated set-up including a high vacuum irradiation chamber is needed, typically with pressures below 10^{-6} Pa. They are usually equipped with a cryostat (bath or continuous flow). Liquid nitrogen (T= 77 K) is well suited to simulate Solar System temperatures. Often, with a closed-cycle helium cryostat temperatures below 10 K can be reached. With a suitable heating system (resistive), a temperature range from around 10 K to room temperature 300 K can be investigated. This allows covering different space regions, from the "snow line" to the outer Solar System and beyond including very cold ISM regions (dense molecular clouds). It may also be interesting to slowly evaporate volatile gases and to obtain a room temperature residue for further analysis.

The preparation of the sample is often done by condensing gas phase molecules in-situ on a suitable substrate, the nature of which depends on the chosen analysis method. In some cases (organic molecules) it is also possible to prepare a thin layer *ex-situ*. Deposition of one specific molecule (pure H_2O for example) is possible, but also mixtures or co-deposition of two or more different molecules. A very low base pressure (below 10^{-8} Pa) is required to avoid contamination from the residual gas or deposition (in particular, of water molecules) during irradiation and analysis. Finally, a multitude of methods of analysis are available to study how the specimens evolve when irradiated (see 2.1).

Figure 2 shows schematically a typical ion irradiation set-up for ices at low temperatures. The ion beam impinges on a thin sample prepared on a cold substrate (here an IR transparent window), which is analysed (in this example) by Fourier Transform Infrared absorption spectroscopy FTIR.

2.1 Ion sources and accelerators

The most widely used basic sources for a charged particle beam are electron guns. They appear in many fields of applications including cathode ray tubes, electron microscopes and particle accelerators, to name a few. Electrons emitted from a cathode are accelerated by electrostatic fields and focused by dedicated lenses. The cathode most often is a hot filament as in a light bulb, or an indirectly heated emissive layer. Electron guns cover a wide range of energies, form a few eV to some tens of keV (cathode ray tubes), and up to some hundred keV (microscopes, irradiation devices). Those low to medium energy guns are useful in studies of interaction of ionising radiation with astrophysical ices. We mention that electrons accelerated to higher energies can be useful in the field of laboratory astrophysics, since they can produce UV photons due to synchrotron radiation.

Low energy electrons (typically around 100 eV) can efficiently ionise molecules in the gas phase and serve to create a plasma, from which ions can be extracted by electric fields. This simple principle is used for low energy ion guns delivering singly charged ions which are commercially widely available, e.g. for sputter cleaning, surface structuring, deposition, SIMS (see section 2.2.4)

and so on, with energies up to some tens of keV. Such guns, which affect the very surface and top-most layers of the samples only, are useful to simulate slow ions (solar wind). Another simple source for low energy ions with low charge states is a plasma discharge. In a more advanced design, a plasma created by injected ionising electrons is confined in a magnetic field and ions are extracted by electric fields.

With the advent of the silicon based semiconductor industry, ion implanters became most important for modifying the properties and structure of silicon starting in the 70's and 80's. Implantation depths up to microns can be reached. At that time also the widely used numerical simulations of ion interaction with solids such as SRIM (Ziegler, Biersack and Ziegler 2008) were developed because of the needs of the semiconductor industry. In astrophysical simulations, implanters allow experiments with light ions (hydrogen, helium) in the electronic energy loss regime. It is important to note that also heavier ions, where nuclear energy loss may prevail and which can easily be produced in simple ion sources (C, N, O, Ne, Ar), have been accelerated and widely used in astrophysical laboratory simulations.

Higher energy accelerators emerged with the advent of nuclear physics, triggered by discoveries using what we could call "natural accelerators" such as radioactive sources. As an example, alpha emitters allowed Rutherford's famous experiment using the scattering of alpha particles to discover the structure of atoms and giving access to the dimensions of the atomic nucleus. Also, the fission fragments discussed as heavy charged particle source in section 2.2.5 come from "natural acceleration", and even cosmic rays can be counted to this class. Nevertheless, laboratory accelerators have a major advantage: they deliver beams with well defined projectile mass, charge state and energy. A short overview on accelerators is given by Spohr (1990) and more detailed information on particle accelerators can e.g. be found in Wille (2001).

Large electrostatic accelerators such as the Cockcroft-Walton and the Van de Graaff (VdG) devices, named after their inventors, were developed starting in the late 1920's. The history of accelerator development in nuclear physics is nicely covered by Sessler and Wilson (2007). The Cockroft-Walton is based on high voltage rectifier units converting AC to DC current. Cascades of diodes and capacitor stages can be assembled to make a voltage multiplier (for detailed description see Scharf 1986). The VdG uses an electrostatic charging belt (or chain) to transport charge to the spherical high voltage terminal containing the ion source. In the first prototype, charge was sprayed upon a silk belt. The high voltage terminal reaches a potential, and ions from the source travel through a tube under vacuum inside an acceleration column. The gained kinetic energy depends on the charge state q when being accelerated from high voltage (U) to ground (0): $E = q\,U$. This already shows the interest in developing highly charged ion sources for technical reasons in addition to scientific interest in high charge effects. The first electrostatic accelerators were mounted in air which strongly limits the achievable terminal voltage to typically some hundred MV. To overcome this breakdown limit, the high voltage terminal with the ion source, the belt, the tube and column usually are mounted inside a

tank filled with e.g. SF_6 gas at high pressure. Terminal voltages of more than 20 MV have been reached in this way. However, the most widely used small VdG machines have a terminal voltage of about 2 MV. Not only atomic ions, but also cluster ions and electrons can be accelerated in this way.

Higher energies can be achieved by using the tandem principle, where the terminal voltage is used twice to accelerate the projectiles. An ion source on ground potential delivers negatively charged ions which travel to the terminal and gain a kinetic energy of E = U. They are stripped of their electrons by a gas stripper or a thin foil and then again gain the additional kinetic energy E = q U.

The next step to achieve even higher energies was the invention of the cyclotron by Ernest O. Lawrence in 1932: e.g., see the review by Sessler and Wilson (2007). The basic ideas are to change the geometry from linear to circular and to go from electrostatic fields to high frequency acceleration. The projectile ions are guided by a magnetic field on circular trajectories. The acceleration happens when they travel through a gap between two high frequency electrodes. Every time this gap passed, they gain an energy of E = q U and thus E = n q U after n passages. Also, the radius of their trajectory increases and therefore the revolution frequency remains constant allowing to use a fixed high frequency. Cyclotrons are used e.g. at GANIL, where successive acceleration by three cyclotrons makes it possible to do experiments with projectiles of approximately 1 MeV/u, 10 MeV/u and 100 MeV/u. This covers a wide range of the electronic energy loss below, around and above the maximum of the electronic stopping power domain (Figure 1), and thus permits a meaningful laboratory simulation of cosmic ray effects**.** The corresponding penetration depths (ranges) are of the order of some micron to several mm in condensed matter.

In contrast to cyclotrons, synchrotrons rely on time varying magnetic fields, while the particles travel on a circular orbit of constant radius. The most energetic nuclear and particle physics experiments rely on synchrotrons. Among the linear accelerators based on high frequency fields, we mention the radio frequency quadrupole (RFQ) which mainly work at energies around 1 MeV/u. They are nowadays widely used, often as injectors, in connection with highly charged ion sources such as ECR sources.

These "electron cyclotron resonance" sources make use of a "magnetic bottle" (a suitably shape magnetic field) to confine a plasma made from a low density gas ionised by microwave radiation. Permanent magnets make these sources relatively small and reliable so that they can also be used in ion beam therapy of cancers. It is also possible to produce e.g. beams from metallic sources, such as Fe, by introducing particles sputtered from a solid in the plasma of a carrier gas. Such sources not only serve for high energy accelerators, but are widely used in atomic collision and surface physics and other domains. They can e.g. be used to study the effects related to the potential energy of the projectile (section 3), and for delivering intense beams of heavy ions for low energy implantation studies (section 6). For more information about ion sources, see Brown (2004).

We finally mention that often, in order to obtain a homogenous dose distribution, the beams are swept over the sample surface. An important point is also the dosimetry, since the deposited dose

is related to the accumulated exposure time of objects in space. The ageing of such objects over millions of years can be simulated by irradiation in the laboratory during hours or days. Heavy ions, which may deposit energy at a much higher rate than protons (Figure 1) may thus present an advantage in this respect. However, specific effects such as multiple ionisation occur with heavy ions (see Rothard and Gervais 2006, and references therein). The fluence (number of incoming projectiles per cm^2) has to be determined with sufficient precision if sputter yields or cross sections are to be determined. This is in most cases done by current measurements: the current at a suitable collimator upstream is measured to monitor the projectile flux during the irradiation. A Faraday cup can be inserted before and after irradiation to measure the projectile current.

2.2 Detection techniques

They include optical methods (most often Fourier Transform Infrared Absorption FTIR, but also UV-visible and Raman spectroscopy) and the measurement of ejected particles. The methods in the latter case include measurement of total yields via mass loss with a Quartz Crystal Microbalance (QCM) or the catcher technique (where ejected particles stick on a suitable catcher and the number of particles per unit area is measured e.g. by Elastic Recoil Ion Analysis (ERDA) or Rutherford Backscattering Spectroscopy (RBS) (Assmann, Toulemonde and Trautmann 2007). Identification of ejected particles can be achieved by mass spectrometry of secondary ions (SIMS) or of post-ionised neutrals e.g. with a quadrupole mass spectrometer QMS or Time of Flight measurements (TOF-SIMS). If formation of complex organic molecules is to be studied, *ex-situ* chromatographic analysis of thick residues after slow warming-up of irradiation processed ices is useful. It is safe to say that IR spectroscopy still is the "working horse" of laboratory astrochemistry, but a variety of other techniques is emerging as reviewed recently by Allodi *et al* (2013).

2.2.1 Infrared Absorption Spectroscopy. Spectroscopic techniques are mandatory in experiments oriented toward astrophysical applications, as most, sometimes all, of the information we get from astrophysical objects arise from remote observations with satellites and telescopes. In this respect infrared spectroscopy plays an important role in astronomy and laboratory experiments. The covered domain is adequate to follow the vibrational modes absorptions in molecules, radicals and solids, and is used to identify and monitor physical and chemical evolution of interstellar ice mantles, either observed or simulated experimentally. In addition, these mantles often occur in interstellar regions opaque to be probed by ultraviolet or visible (UV-vis) radiations. Most modern experiments are based on Fourier transform infrared spectrometers, coupled directly to the vacuum chamber via an interface IR-transmitting window, and the composition and evolution of the samples can be followed in situ while irradiated. The technique is usually sensitive to monolayers of molecules up to several microns thick samples, in adequacy with typical astrophysical observations.

An example of FTIR spectra is shown in Figure 3. A Spectrum for unirradiated CO_2 ice is compared to a spectrum taken after irradiation with $^{50}Ti^{21+}$ ions of 11.4 MeV/u at a projectile fluence of $1.65x10^{13}$ ions cm^{-2}. In the "as deposited" spectrum, IR absorption lines of CO_2 are observed (both naturally abundant isotopes ^{12}C and ^{13}C appear). After irradiation, the daughter molecules CO, CO_3 and O_3 appear. From the peak intensity and the absorption strength (A-Value), the column density of the molecules can be calculated and analysed as a function of projectile fluence (see section 5.3 and Figure 7).

2.2.2 UV-Vis spectroscopy. Although ultraviolet-visible spectroscopy is a powerful laboratory technique to detect specific molecules via their electronic transitions, it is not of practical use in the study of the ice mantles in the ISM. The reason is that ices can form only when the clouds are dense enough but this implies they often completely absorb the UV-Vis radiation of the stellar sources. Such a spectral range is, however, fundamental in the study of the extinction curve of the diffuse clouds where ices are not accreted and the dust is dominated by sub-micrometer sized silicates and carbons. Particularly interesting is the study of carbonaceous materials believed to be responsible for the extinction bump at about 217.5 nm and for the far-ultraviolet rise (e.g. Fitzpatrick and Massa 2007, Gavilan *et al* 2016 and references therein). The case is different for the ices in the Solar System, particularly for the icy satellites of the giant planets (Jupiter, Saturn, and Uranus). Of the greatest relevance are in fact observations in the UV range (200-320 nm) that allowed identifying specific molecules such as sulfur dioxide and ozone (for a review see Hendrix *et al* 2013).

Nevertheless, few are the laboratory experiments that use UV-Vis spectroscopy to investigate the effects of energetic processing of ices (see e.g. Sack *et al* 1991; Teolis *et al* 2006; Jones *et al* 2014a,b).

2.2.3 Raman spectroscopy. Raman spectroscopy is a very powerful technique, considered complementary to the IR spectroscopy, to investigate, in particular, the structural properties of the sample and has often been used to study the effects of ion induced lattice damage in carbonaceous solids (e.g., Elman *et al* 1981; Strazzulla and Baratta 1992; Baratta *et al* 1996; Kalish *et al* 1999; Strazzulla *et al* 2001; Constantini *et al* 2002). It has also been used in the laboratory to evidence the formation of polyynes that are difficult to identify in the infrared after ion bombardment of frozen hydrocarbons (Compagnini *et al* 2009; Puglisi *et al* 2014).

2.2.4 TOF-SIMS. Particles sputtered from the surface (see section 3) may be used as a tool to monitor radiation effects. A certain number of techniques have been developed for this purpose (Behrisch *et al* 2007). Concerning astrophysical ices, "Secondary Ion Mass Spectroscopy" (SIMS) using quadrupole mass spectrometers (QMS) or the measurement of the "time of flight" (TOF) of ejected particles allow to record mass spectra of ejected particles. Post-ionisation by electrons beams or lasers allows

extending the methods to neutral ejecta. Indeed, only a fraction of ejected particles are charged, of the order of 10^{-1} to 10^{-6} with respect to neutrals depending on the projectile combination, impact energy, target composition and structure. In cases relevant to astrophysics, ionised particle yields of the same magnitude as that of neutrals have been reported, demonstrating the usefulness of ionic particles as information about surface stoichiometry (Dukes *et al* 2011). These techniques allow measuring mass resolved partial sputter yields and of energy distributions.

By construction, the TOF-SIMS technique requires a pulsed projectile ion beam. The time interval between the impact of a single projectile (or a bunch of projectile ions) on the sample and the arrival of the emitted secondary ion in a detector at a given distance of the sample is used to determine the mass of the secondary ion (Stephens 1946). The pulsed beam is obtained by fast variation of electric potentials in deflection plates or of the accelerating electric fields between electrodes. As a result, periodic eV- keV ion beams are produced (Benninghoven 1969). MeV ion accelerators, such as the Van de Graaff electrostatic-type (Della Negra *et al* 1983, Sundqvist 1992) re-accelerate the pulsed ion beams delivered by the ion source. Beams delivered by certain types of accelerators are already pulsed, such as e. g. the GeV cyclotrons of GSI (Wien *et al* 1991) and of GANIL (Hijazi *et al* 2011, Martinez *et al* 2015).

Sufficiently low intensity beams allow a quasi-non-destructive analysis not significantly altering the specimen during measurement ("static SIMS"). In contrast, "dynamic SIMS" measurements are made during irradiation with rather high currents and the evolution with fluence is recorded for selected masses (QMS). A TOF measurement can be combined with imaging XY detection of the impacting secondary ion. The improvement to conventional TOF-SIMS is that now three quantities (TOF and two positions X and Y) are measured, i.e. the complete velocity vector. In addition to mass distributions, differential yields such as angular distributions or energy spectra can be determined (Allodi *et al* 2013). Differential (energy, angle) XY-TOF-SIMS studies have been conducted only in some select cases such as distributions of H^+ and H^- sputtered from water ices (Iza *et al* 2007).

TOF-SIMS measurements can complete FTIR as discussed by Andrade *et al* (2012). For example, information about species which cannot be directly observed by IR spectroscopy (symmetrical molecules such as H_2, N_2, O_2) can be obtained. IR spectroscopy probes the bulk of the samples, whereas TOF-SIMS is sensitive to the surface. Furthermore, the observed ejected particles are instantaneous messengers of the induced processes.

2.2.5 The ^{252}Cf-PDMS technique. In the 1970's, a new method based on stochastically pulsed MeV ions was developed, aiming the employment of the ion desorption process not for physics surface analysis but rather as a chemical and biochemical analytical tool (Macfarlane and Torgerson 1976). This technique - called Plasma Desorption Mass Spectrometry (PDMS) - used initially a radioactive alpha source (for producing MeV helium ions) which was quickly replaced by a ^{252}Cf fission fragment

(FF) source (Busch and Cooks 1982), since the ion desorption yield increases as a power of the projectile charge state (Barros Leite *et al* 1992). Typical ^{252}Cf FF are ^{108}Tc and ^{144}Cs, with charge states around 20^{+}. At that time, it was already clear that high energy heavy ions should be the best projectiles to induce efficient emission of secondary ions; FF are two orders of magnitude more efficient than MeV light ions produced by MV accelerators for transferring energy to the solid surface (Collado *et al* 2004, Farenzena *et al* 2005a). The fact that the source emits FF with large mass and velocity distributions is not a major problem for analytical purposes. An example of TOF-SIMS spectra is shown and discussed below (section 3, Figure 4).

The advantages of ^{252}Cf-PDMS over ion sources and accelerators are: i) the production of 100 MeV FF is relatively inexpensive; ii) small size ion source (mm): it may be placed very near to the sample; iii) the emitted average FF flux is constant for practical applications (the ^{252}Cf half-life is 2.6 years); no ion optical devices; iv) the fact that a pair of fission fragments is always emitted during the nuclear fission event allows a convenient coincidence-method for thick sample analysis (one fragment induces the ion emission, the other one triggers the electronics). It should be emphasized that it is only possible to detect secondary ions (positively or negatively charged) with the standard PDMS setups; but not sputtering yields of neutrals. Because secondary ion emission is very fast (~ps), the atomic and molecular species emitted are those corresponding to the first generations of ions formed just after the projectile impact. PDMS is well suited as fast analysis tool, but accelerators are better options for experiments requiring a dedicated simulation with defined projectiles mass, charge state and energy, and if high fluences (energy deposition) are needed.

3. Sputtering: cascades and electronic excitation

Besides radiolysis and creation of defects, the sputtering of atoms and molecules from the surface of condensed matter occurs driven by various mechanisms (Behrisch and Eckstein 2007). At low projectile velocities (when S_n is dominant) knock-on sputtering from elastic collision with the target nuclei prevails as described by Sigmund's theory (linear collision cascade, Sigmund 1969). For a swift ion (S_e dominant, inelastic collisions with the target electrons) the so-called "electronic sputtering" occurs. Proposed models to describe electronic sputtering include "Coulomb explosion" (Fleischer, Price and Walker 1965) and the widely used "thermal spike" model (Seitz and Köhler 1956). It is assumed that the energy deposited on the electronic sub-system is transferred via electron-phonon scattering to the ionic grid resulting in a temperature increase, which can lead to track creation above the fusion temperature, and to particle ejection above the sublimation temperature (Assmann, Toulemonde and Trautmann 2007). With low velocity, sufficiently highly charged ions, a contribution of "potential sputtering" may occur due to the potential energy leading to electron capture and local excitation of the material. Subsequently, excitons may be formed, trapped and be involved in "defect mediated sputtering" (Aumayr and Winter 2004).

In the interstellar medium, electronic sputtering is one of the processes at work injecting species in the gas phase from the interaction of cosmic rays with dust grains, in addition to other mechanisms such as stochastic heating and CR-induced photodesorption of secondary photons. In shielded regions, the release of molecules from ice mantles via sputtering has a potential impact on the gas phase abundances, especially for species efficiently sticking at low temperature.

Low energy electronic sputtering has been investigated experimentally in the laboratory since a long time within an astrophysical context covering both planetary ice context and extrapolated with scaling laws to higher energies for interstellar ices (e.g. Brown *et al* 1984; Ellegaard *et al* 1994; Johnson and Schou 1993; Bahr *et al* 2001; Baragiola *et al* 2003; Plainaki *et al* 2012 and upward citations). Recently, measurements were extended to the sputtering yield (molecules per incoming projectile) for simple ices to larger energies and heavier ions (Seperuelo *et al* 2009, 2010; Dartois *et al* 2013, 2015a,b, Mejia *et al* 2015b). Important consequences in astrophysical environments are the contribution of sputtering to the desorption from grains in molecular clouds and, in the Solar System, formation of planets and satellites exospheres.

3.1 The exospheres of icy satellites

The proof of the existence and the characterization of tenuous atmospheres, referred to as exospheres being the molecules gravitationally bounded but not interacting, of some icy satellites have been obtained by several space missions the most recent being Galileo and Cassini (e.g. Barth *et al* 1997, Hansen *et al* 2005). The observations have been modelled on the basis of laboratory results demonstrating that the main process that produces exospheres is sputtering by keV-MeV ions from the magnetospheres (Johnson 1990; Plainaki *et al* 2013).

The most studied among the exospheres is that of Europa: the most abundant molecule sputtered from the surface is H_2O followed by the products of water radiolysis, mainly H_2 and O_2 along with minor amounts of water radicals (O, H, OH). Also, no-water products and trace species such as Na or K are released (e.g. Cassidy *et al* 2009). Water molecules efficiently freeze out at the local temperatures and most of them do not have sufficient energy to escape from Europa's gravity, whereas H_2 is not gravitationally bound and is preferentially lost. Consequently, O_2 is believed to be the dominant atmospheric constituent (e.g. Shematovich *et al* 2005; Smyth and Marconi 2006). This view, however, has been recently questioned by Shemansky *et al* (2014), who after re-analysing data from the Cassini Ultraviolet Imaging Spectrograph, conclude that the atmosphere at Europa is dominated by atomic oxygen at a density two orders of magnitude below the previous O_2 estimate.

3.2 Origin of gas phase molecules in dense clouds

In the electronic stopping regime, a strong non-linear increase of sputtering yields Y with deposited energy is observed. For O_2, N_2, CO, CO_2 and H_2O, a quadratic dependence with the electronic stopping power, $Y \sim S_e^2$ was observed with both light ions (H, He) and with heavy ions (Boduch *et al*

2015, Dartois *et al* 2015a) as shown in Figure 4. If the energy of the projectiles is high enough and the ions are almost completely stripped, $S_e \sim Z_p^2$ resulting in an extremely strong dependence $Y \sim Z_p^4$. This strong dependence can compensate largely for the several orders of magnitude lower abundance of heavy ions in cosmic rays. Therefore, the total amount of sputtered molecules is higher than that desorbed only by the more abundant protons, and heavy ions also are rather competitive compared to photodesorption.

This experimental observation may help understanding the evolution of dense molecular clouds, where one would expect that with the exception of hydrogen all molecules should condense on small grains due to the extremely low temperature (10 K) within timescales of $\sim 10^9/n_H$ years (n_H is the number density of hydrogen). This comes out to be much shorter than the lifetime of the clouds of a few million years (e.g. Elmegreen 2007, Mouschovias *et al* 2006). However, e.g. CO molecules are observed in the gas phase. As major processes to explain the gas phase molecules, photodesorption from ices by secondary UV photons from cosmic ray interaction with hydrogen and "spot heating" of grains were evoked (Léger, Jura and Omont 1985, Öberg *et al* 2007). This latter process must not be confused with the electronic sputtering discussed above. Deep inside dense clouds, each of the three processes (electronic sputtering by the heavy ion fraction of cosmic rays, "spot heating" of grains by cosmic rays, photodesorption) yield comparable contributions to the total desorption yields (Seperuelo *et al* 2010).

It is important to note that the target thickness dependence of electronic sputtering of thin films is pertinent to e.g. thin ice layers on grains. With different condensed molecules like frozen solid argon (Johnson and Schou 1993) and CO_2 (Mejia *et al* 2015b), an increase of sputter yields with layer thickness was reported. A constant "thick ice layer" yield was observed with frozen argon at about 0.1 μm which corresponds to the typical maximum ice layer thickness on interstellar dust grains. However, solid argon is specific as a rare gas, the deposited electronic energy may be dissipated differently than in other ices, so this may not be a general finding. Possibly, due to substrate effects, even an increase could be possible for thin layers.

3.3 ^{252}Cf-PDMS results on astrophysical ices

Considering that sputtering is a relevant process occurring continuously in space for any solid body exposed to cosmic rays, stellar winds and to particles trapped in planetary magnetospheres, and that ^{252}Cf-PDMS is a suitable and practical technique for the analysis of ion desorption, many astrophysical icy systems have been investigated this way.

The study of ices by PDMS was pioneered by K. Wien and collaborators (Hilf *et al* 1993, Wagner *et al* 1993). They reported an interesting characteristic of the negative C_nH_m ions emitted from alkane and benzene ices, which were found to be stable if $m \leq 3$ only. This property was also observed for other hydrocarbons (Betts, da Silveira and Schweikert 1995) and explained theoretically

(Fantuzzi *et al* 2013); it may have consequences for carbon rich materials enveloping comets and ice grains.

A systematic study of ices by PDMS was initiated by Collado *et al* (2004), and a first review can be found in Farenzena *et al* (2005a). The following ices have so far been analyzed: H_2O (Collado *et al* 2004, de Barros *et al* 2011b), CO and CO_2 (Farenzena *et al* 2005b,2006 Ponciano *et al* 2005, 2006 NH_3 and NH_3+CO (Ponciano *et al* 2006, Martinez *et al* 2007a, 2007b, 2014), HCOOH (Andrade *et al* 2007), N_2 and N_2+O_2 (Fernández-Lima *et al* 2007, Ponciano *et al* 2008), H_3COH (Andrade *et al* 2009). Most of the measurements have been made at 25 K. The effects of the ~ 65 MeV heavy ion projectiles, which concerning electronic energy deposition mimic the heavy ion component in particular and cosmic rays in general, on several pristine ices, have been investigated by this method.

To illustrate some of these results, Figure 5 shows positive and negative secondary ions emitted from ammonia ice. The main general conclusions on sputtering of ices which can be drawn are as follows. The TOF analysis of the secondary ions reveals the emission of a very large number of molecular species (clusters). Due to secondary electron emission, the total sputtering yields of positively charged species are higher than the negative ones. In the case of ices, the dependence of the yields of positive and negative cluster ions on their mass is basically the sum of two decreasing exponentials. This is already visible from the rough peak area evolution (plotted in semilog scale) in Figure 5. This phenomenon is due to the cluster formation mechanisms (Farenzena *et al* 2005a, 2005b, 2006).

It is interesting to note that relatively high abundances occur around certain masses as can be seen from the inset of Figure 5. This property is ruled by the stability of each cluster molecular structure, taken into account the stoichiometry of the material. Concerning the comparison of emission of neutral and charged particles, in general, the dominant mechanism of the neutral species sputtering is different from that of ionic species. In particular, yields of neutrals can be orders of magnitude higher than those of secondary ions; the dependence of the total yield of neutrals on the stopping power S_e follows a square dependence with the electronic stopping power, $Y \sim S_e^2$ (Figure 4), while that of secondary ions increases with the third power $Y \sim S_e^3$ (de Barros *et al* 2011c).

4. Modification of the structure: compaction and amorphisation

Ion irradiation produces modification of the physical state of the ice i.e. its structure (crystalline versus amorphous, porous versus compact) of the irradiated samples, often neglected compared to radiolysis induced chemical modification. Nevertheless, this is important in many aspects for astrophysics. The structure of water ice depends also on the temperature. It is amorphous if deposited at low temperature (10-30 K) or crystalline if the deposition temperature is higher than 140-150 K. The crystalline structure is stable against temperature cycling, but it is amorphised if the ice is subjected to energetic processing by e.g. ion bombardment. Also, porous ice can be compacted by irradiation.

The efficiency of amorphisation and compaction can be quantified by the corresponding cross sections. To interpret observations and give input to physico-chemical models relevant to astrophysics requires constraining the evolution of ice under irradiation and their influence on the structure, it is necessary to know how the cross sections scale with the amount of deposited energy. This allows for example to estimate the time needed for crystalline ice to become amorphous (or porous ice to become compact) if exposed to a certain radiation field (e.g. that of cosmic rays or magnetosphere ions). The topic has been under discussion for some time (Baratta et al. 1991, Moore and Hudson 1992, Leto and Baratta 2003, Palumbo 2006, Raut et al. 2007, Palumbo et al. 2010) and recently found new interest with the advent of swift heavy ion irradiation allowing to establish scaling laws for compaction and amorphisation (Dartois *et al* 2013a; Mejia *et al* 2015a; Dartois *et al* 2015a,b; de Barros *et al.,* 2016).

4.1. Icy satellites

The icy surfaces of the satellites of the giant planets in the outer Solar System exhibit a variety of ice structures (Grundy *et al* 1999) believed to be due to the competition between crystallization (thermal processing) and amorphisation (energetic processing), see e.g. Dalton *et al* (2010). Particularly interesting is the comparison of the three major Jovian icy satellites. Ice is mostly amorphous on the surface of Europa where the temperature is lower and ion fluxes are high and crystalline on Callisto that has the highest temperature.

Both structures are found on Ganymede (Hansen and McCord 2004). Roughly, the distribution of crystalline and amorphous surface ice on Ganymede is consistent with the expected distribution of energetic magnetospheric ions, although there are not yet enough spatially resolved data to confirm the relation between the local fluxes of energetic particles and the structure of the ice.

4.2. Water ice on dust grains in the ISM

Water ice, the main constituent of ice mantles, may be present as amorphous solid water (ASW) phase with open porosity at the low temperature of dust grains in the interstellar medium (~10 K). In infrared spectra, the appearance of non hydrogen-bonded OH water ice molecule signatures is the first indication of such a porous structure. It gives rise to so-called OH dangling bonds (OH-db) with 2 or 3 molecules coordination (Buch and Devlin 1991, Palumbo et al 2010) at 3720 cm-1 and 3695 cm-1.
The intensity and evolution of the OH-db under ion irradiation as a function of projectile fluence yields information on the degree of pore compaction. The presence of porous ice influences surface chemistry in space, since the surface available for chemical reactions to take place is larger in this case than for more compact ice.

Thus, CRs induce structural ice modification. The corresponding evolution of (most often water) ices has been studied since about 30 years mainly at low energy and with light ions (Baratta *et al* 1991, Strazzulla *et al* 1992, Moore *et al* 1992, Roser *et al* 2002, Leto and Baratta 2003, Baragiola *et al* 2003, Mastrapa *et al* 2005, Palumbo 2006, Raut *et al* 2006, Raut 2008, Fama 2010, Palumbo *et al*

2010). In such studies, a fresh water ice film was condensed in vacuum from the gas phase on a cold window at low temperature. The IR spectrum of the OH-db was followed as a function of projectile fluence. The analysis allows deducing a low energy compaction cross-section. Other techniques using optical measurements can also be performed. Nevertheless, with respect to astrophysics, IR spectroscopy has the advantage that it can be compared to space observations. The porous amorphous ice phase obtained is getting compacted under ion irradiation and finally evolves towards a compact non-porous, but disordered amorphous phase (Palumbo 2006).

From the main OH stretching mode band of water ice at about 3300 cm^{-1} (λ~3μm), other observational constrain can be obtained. The experimentally observed disappearance of the ASW OH-db bonds is indeed accompanied by a change of the main OH band's profile. Furthermore, an increase of the associated integrated band strength occurs due to restructuration and pore collapse. Such observations were reported for swift heavy ion (SHI) irradiation (Mejia *et al* 2015a). The cross-sections deduced from the observation of the main OH band are close to that measured via the evolution of the OH-db. Also, the central position of the stretching mode band can be monitored as a function of projectile fluence fluence for different initial ice mixtures to be finally compared to astronomical observations. The results for ice mixtures are compatible with the observations obtained with pure water ice OH-dbs. However, this procedure is less constraining, because other factors may come into play that influence the band centre. Examples are compositional changes or optical effects due to grain shapes, which could slightly displace the centroid of this intense band.

The compaction cross section scaling reported by Dartois *et al* (2013a) as a function of electronic energy loss combining experiments with light ions and high energy heavy ions covers three orders of magnitude. The relevant compaction time scale for the ice network on icy mantles covering interstellar dust grains in dense molecular clouds of our galaxy was estimated to fall in the range from 1.4×10^5 to 2×10^6 years, small compared to cloud lifetimes. The used astrophysical model includes the expected galactic cosmic ray distribution of ion abundances and reproduces the ionisation rate observed (Dartois *et al* 2013a, Dartois *et al* 2015a).

It is also possible to follow the change of the stretching mode profile irradiating a crystalline water ice film maintained at the same low temperature as the above discussed ASW. In the case of crystalline ice, a strong change of the profile and a decrease of the integrated band strength of the ice is observed as consequence of SHI-induced amorphisation. The compaction and amorphisation doses are about 1 eV/molecule and 3 eV/molecule, respectively. From the infrared spectra, it can be deduced that the same final amorphous compact state is reached starting from ASW (Leto and Baratta 2003; Dartois *et al* 2013a; Mejia *et al* 2015a) or crystalline ice. However, the ion-induced phase change cross-section is lower for crystalline ice by about a factor of three (Dartois *et al* 2015a,b), the latter being intrinsically more resistant to the transformation.

5. Radiolysis and formation of new molecular species

Excitation or ionisation of molecules by ionising radiation can lead to their fragmentation (radiolysis). In this respect, heavy ions are an order of magnitude more efficient in destroying the initial molecules, when molecule destruction yield are normalized to the deposited energy, i.e. the corresponding radiochemical yields G are much higher than that of protons (or ionising photons like UV and X-rays). With condensed layers containing several simple molecules, radiolysis and the following chemical reactions become more complex and there is a trend toward chemical complexity possibly leading to the synthesis of organic and pre-biotic molecules (e.g. Ehrenfreund *et al* 2002).

5.1. Radiolysis of icy satellites

As said the surfaces of many icy satellites are dominated by water ice and hydrated materials (e.g. sulfuric acid). Minor amounts of other species such as H_2O_2, SO_2, and CO_2 and organic compounds are also observed. However, the number of compounds present at the surface (and below) is higher than observable by spectroscopic techniques. This is testified by the observation of a large number of gaseous species in the exospheres and in particular in the plumes of Enceladus (Waite et al. 2009) that include H_2CO, nitrogen bearing species (NH_3, N_2, HCN) and hydrocarbons. Irradiation by the abundant fluxes of energetic ions and electrons (Bennett, Pirim and Orlando 2013 and references therein) drive a chemical evolution (radiolysis) that could have produced some of the observed species and others that have not yet been observed in the solid and/or in the gas phase (Strazzulla 2011).

An example of the radiolytic effects is the synthesis of hydrogen peroxide, which has been found on the surface of Europa (Carlson *et al* 1999), Ganymede and Callisto (Hendrix *et al* 1999). Several groups have studied the formation of hydrogen peroxide by ion bombardment of water ice (Moore and Hudson 2000; Gomis *et al* 2004; Loeffler *et al* 2006). There is a large agreement on the fact that its presence on the surfaces of icy satellites is evidence of radiolysis. It would, however, be extremely important to obtain detailed surface maps of hydrogen peroxide and other oxidants to be related to the local flux of energetic ions and electrons. This information would be important also because it has been suggested that oxidants produced at the surface can diffuse in the underneath layers, reach the ocean and furnish the chemical energy necessary to maintain a biosphere (e.g. Chyba 2000).

There is also a large consensus on the fact that radiolysis is the most relevant driving mechanism for the so called carbon and sulfur cycles (Johnson et al. 2004). In fact, carbon is present as CO_2, and in the form of some kind of elemental and organic carbon. The latter is responsible for an absorption around 4.62 μm attributed to CN groups. Sulfur is present as SO_2, sulfuric acid (and possibly sulfates), and elemental sulfur. While it is an open question to understand if those compounds are native of the satellites or come from external sources (e.g. micrometeoritic deliveries, ion implantation) there is consensus that radiolysis plays an essential role in cyclically converting one species into another.

Numerous studies have been conducted on the radiolysis of sulfur bearing species. Loeffler *et al* (2011) have irradiated pure sulfuric acid and sulfuric acid (mono- and tetrahydrated) showing that the monohydrate is the most stable form and can remain on the surface of Europa over geological times. This result has been further strengthened by annealing experiments of crystalline sulfuric acid mono- and tetra-hydrates (Loeffler and Hudson 2012). These experiments showed that post-irradiation heating regenerates the original hydrates. This thermal processing was nearly 100% efficient, indicating that over geological times, thermally-induced phase transitions enhanced by temperature fluctuations will reform a large fraction of crystalline hydrated sulfuric acid initially having been destroyed by radiation processing. At the same time, sulfur implantation experiments (see section 6 for details) have demonstrated the efficient formation of hydrated sulfuric acid (Strazzulla *et al* 2007, Ding *et al* 2013).

A large number of experiments on frozen H_2O:CO_2 mixtures in different abundance ratios irradiated by energetic ions and electrons in a very wide range of energies (Boduch *et al* 2011; Gerakines *et al* 2000; Jones *et al* 2014a, Peeters *et al* 2010; Pilling *et al* 2010b; Zheng and Kaiser 2007; Strazzulla *et al* 2005) have demonstrated the formation of abundant oxidants such as ozone, carbonic acid and hydrogen peroxide as well. This could be a first step in further chemical evolution particularly where additional icy species are present as those cited above.

Here we wish to quote also the results of recent experiments of electron bombardment of pure carbonic acid. The techniques IR, UV-Vis and mass spectrometric were used and evidenced the re-formation of water and carbon dioxide (Jones *et al* 2014b). A particularly interesting finding is that the re-formed CO_2 is embedded in the carbonic acid has a 4.27 μm band whose profile (peak position and FWHM) well reproduces that observed on the surfaces of Callisto and Ganymede (Jones *et al* 2014b) and previously attributed to CO_2 in a not identified non-ice material (Hibbitts *et al* 2002, 2003).

5.2. Space weathering

The cumulative effects of irradiation by solar ion populations (solar wind, flares, solar energetic particles events), galactic cosmic rays, electrons, UV and X-rays, and bombardment by micrometeorites are known as space weathering (SW). In addition to the chemical and structural effects described above, SW causes changes in the optical properties, in particular the spectral slopes (colors) of the surfaces of the minor, airless, bodies in the Solar System. These minor bodies include rock-dominated asteroids that populate the main belt (a region between the orbit of Mars and Jupiter) while others that orbit near the Earth are known as NEOs (Near Earth Objects). Excellent reviews have been published recently on this subject (Gaffey 2010, Bennett, Pirim and Orlando 2013, Brunetto *et al* 2015).

Here we are interested to airless bodies whose surfaces are dominated by frozen gases. As said above they can be roughly divided in water ice dominated (as e.g. many satellites of the giant planets Jupiter, Saturn, and Uranus), and colder objects whose surfaces are rich in more volatile frozen gases

(CO, CO_2, N_2, CH_4, CH_3OH, etc.) and may or may not exhibit water ice features. These bodies include the dwarf planet Pluto, Neptune's satellites, the TNOs and comets in the Oort cloud.

The results obtained in laboratory experiments have demonstrated the formation of refractory residues after ion bombardment of hydrocarbon rich mixtures and have been used to predict the development of a refractory organic crust that inhibits a direct exposure of ices at the surface of comets and TNOs (Strazzulla *et al* 1991, Strazzulla *et al* 2003a). These predictions seem to be confirmed by observations such as those presently ongoing for comet 67P/Churyumov-Gerasimenko by the VIRTIS/Rosetta instrument (Capaccioni *et al* 2015). At deeper layers, until about 5 meters depth, the nucleus is depleted in volatiles. It would thus have a considerable fraction of organic molecules formed because of irradiation along with unrecombined radicals (Strazzulla and Johnson 1991). Near the surface, the dose deposited by cosmic ions is high (hundreds of eV/16 u) and decreases with the depth. Doses as low as a few eV/16 u are accumulated at depth of the order of tens of meters.

The development of such materials deeply changes the color of the irradiated surfaces. As an example in Figure 6 we report the reflectance spectra, scaled to 1 at 0.8 μm, of frozen methane as deposited (16 K) and after irradiation with 200 keV H^+ ions at two different doses. The original methane is a transparent solid and its normalized spectrum is consequently flat. Ion bombardment causes a dramatic increase of the spectral slope: the surface reflect less at the lower wavelengths than at the higher (reddening). The spectra of three Centaurus objects (a class of minor bodies orbiting in the outer Solar System) exhibiting different colors (spectral slopes) are also shown in Figure 6. The three objects present different spectral slopes that can be explained as due to the competition of space weathering causing the reddening versus re-surfacing events (e.g. meteoritic impacts) that remove material from the surface and then expose fresh un-weathered materials (Kanuchova *et al* 2012).
It is also important to mention that solid organic materials synthesized by energetic processing of comets can be released as interplanetary dust particles from cometary nuclei when approaching the Sun (e.g. Baratta *et al* 2015) and eventually be found and analyzed on Earth (e.g. Duprat *et al* 2007, Dartois *et al* 2013b).

5.3. Radiolysis of molecules on dust grains by cosmic rays

Irradiation effects with cosmic ray equivalents (electronic energy loss regime) in condensed layers of the simplest and most abundant molecules H_2O, CO, CO_2, NH_3, CH_4 (and also with binary and ternary mixtures) have been extensively studied with light ions. We give some examples without being exhaustive: CO (Palumbo *et al* 2008); CH_4, CO, and N_2-rich mixtures (Moore and Hudson 2003); CH_4 (Baratta *et al* 2003); H_2O:NH_3 (Moore *et al* 2007); H_2O:CO (Hudson and Moore 1999); H_2O:CO_2 (Moore and Khanna 1991); H_2O:hydrocarbon (Hudson and Moore 1998); CH_3OH (Hudson and Moore 2000, Modica and Palumbo 2010); glycolaldehyde and ethylene glycol (Hudson et al. 2005); H_2O:CH_4:N_2, H_2O:CH_4:NH_3 and CH_3OH:N_2 (Kanuchova *et al* 2016).

Our collaboration performed experiments on simple ices with swift heavy ions (Seperuelo-Duarte 2009, 2010; Dartois *et al* 2013; 2015a,b; Mejia *et al* 2015b, Munoz-Caro *et al* 2014, Bordalo *et al* 2013, Pilling *et al* 2013, de Barros *et al* 2011b, Mejia *et al* 2013). The radiolysis of many other ices of somewhat more complex molecules has also been studied with swift heavy ions, among them methanol CH_3OH (de Barros *et al* 2011b, 2014), formic acid HCOOH (Andrade *et al* 2013, Bergantini *et al* 2014), cyclohexane C_6H_{12} (Pilling *et al* 2012) and acetone $(CH_3)_2CO$ (Andrade *et al* 2014).

Figure 7 shows as an example the evolution of the column density N(F) of CO_2 ice (at 20 K) during irradiation with $^{50}Ti^{21+}$ ions (Mejia *et al* 2015b) as a function of projectile fluence F, the number of projectiles that have impacted the target per cm^2. The column density of the initial molecule CO_2 is decreasing. This disappearance of the initial molecule CO_2 is due to fragmentation quantified by a cross section $\sigma(Z,E)$ and sputtering with a yield of Y molecules per incoming projectile. At low fluences, the relative contribution of sputtering to the decrease of N(F) is small for thick enough ice layers. Furthermore, the concentration of radiolysis products (fragments of the initial projectile, new species) can be neglected and at low enough fluence, the projectiles will nearly always impact an un-irradiated region. The decrease then follows an exponential function $N(F) = N_0 \exp(-\sigma F)$ and a best fit to the experimental data allows to deduce the destruction cross section. We note that in some cases for very low fluences at the beginning of irradiation, an apparent increase or anomalous decrease of the column density has been observed. This effect may be related to a change of optical properties due to the compaction (see section 4.2) of the initially porous amorphous ice (Bordalo *et al* 2013, Mejia *et al* 2015a, Dartois *et al* 2013, de Barros *et al* 2016).

During radiolysis, fragments of the initial molecules appear as products. Also, chemical reactions may occur due to recombination of radicals. This leads to formation of new species. In the present simple case of CO_2, the fragment CO and the reaction products CO_3 and O_3 are observed. The column densities of the newly appearing molecules are shown as a function of fluence in Figure 7. They increase up to a maximum value. At low fluence, a simple linear relationship can be used to deduce the formation cross section $\sigma_f(i)$ of each molecular species (i): $Ni(F) \approx \sigma_f(i)\, F\, N_0$. Then, since there will be an equilibrium between production and destruction of these daughters by irradiation, when the sample gets thinner, the column density of the daughters may decrease with fluence (Seperuelo Duarte *et al* 2010, Mejia *et al* 2013).

In many cases, the dependence of cross sections (and also of sputtering yields, see 3.2) was found to follow a simple scaling law: they increase with a power n as a function of the electronic energy loss S_e: $\sigma \sim S_e^n$. The destruction cross sections show variabilities with the species, values of n between 1 and 1.6 have been reported (Bordalo *et al* 2013, Mejia *et al* 2015b, de Barros *et al* 2014a,b). In principle, the formation cross section σ_f of products should follow the same relationship, that is, $\sigma \sim S_e^n$, where n ~3/2; as indeed reported by de Barros et al. 2011b, 2014a.

The so-called radiochemical yields G quantify how many molecules are destroyed or formed per 100eV of deposited energy. They are proportional to the corresponding cross sections dived by the electronic energy loss, $G = 100\ \sigma/S_e$. In Table 1, examples of radiochemical yield values for the destruction of initial molecules (carbon monoxide, methane, methanol, acetone, cyclohexane, and ammonia) obtained with initially pure ices at temperatures T of about 15 K have been compiled. The negative values indicate disappearance, for newly appearing species the values are positive. The formation of the daughter molecules listed in the tables is discussed in the corresponding references.

The values obtained with 220 MeV O^{7+} and different ices (methane, methanol, cyclohexane) show a pronounced dependence on the target molecule. Values obtained with methanol irradiated with different ions very strongly depend on the projectile. Heavy ions are more efficient for a given amount of deposited energy to destroy molecules than light ions. This effect is also useful in ion beam cancer therapy, where e.g. carbon ions have an increased relative biological effectiveness compared to protons (and also photons). In contrast, the G-values for formation of new molecules show a much weaker dependence on the type of projectile (Seperuelo et al 2010, de Barros et al 2011b).

The determination of not only sputtering yields, but also of destruction and formation cross sections is one of the most important goals of such studies, since they allow to establish scaling relations need as input for astrophysical models aiming at estimating e.g. molecular lifetimes (Dartois *et al* 2013, 2015; Kalvans 2015). By including studies with light and a variety of heavy ions it becomes possible to estimate molecular destruction rates for all cosmic ray constituents over a very large energy range. Figure 8 illustrates this procedure for formic acid. First, the electronic stopping power must be calculated with the SRIM software (Ziegler, Biersack and Ziegler 2008) as shown in Figure 1. Introducing the scaling law $\sigma_d \sim S_e^n$ the destruction cross section can be calculated as a function of energy for each projectile. From this and knowing the flux of GCR in the ISM, finally the dissociation rate of frozen formic acid for a distribution of cosmic ray constituents is evaluated. The estimated half-life for the present example of pure formic acid HCOOH in the ISM is predicted to be of the order of 10^8 years (Andrade *et al* 2013, Bergantini *et al* 2014) and one order of magnitude lower, of about 10^7, years for pure acetone $(CH_3)_2CO$ (Andrade *et al* 2014).

We emphasise that chemical evolution may be surprisingly faster with heavy ion cosmic rays than with the more abundant protons and alpha particles: de Barros *et al* (2013) report that the half life time in the ISM of formic acid due to iron bombardment is about 5 times shorter than that induced by protons. For methanol CH_3OH, the half-life time due to iron bombardment is about 10^7 years (de Barros *et al* 2011b) in the ISM; in the Solar System, however, protons from the solar wind have the most important effect.

Occhiogrosso *et al* (2011) have estimated the formation cross section of methyl formate after ion irradiation of CH_3OH-rich ice mixtures at low temperature. This value has been added to a chemical model to investigate the chemical evolution of protostellar objects. They have found that

low-energy cosmic rays interaction with icy grain mantles could explain the abundance of methyl formate observed in dark clouds, such as B1-b core (Öberg *et al* 2010).

As a further example Woods *et al* (2015) have obtained the formation cross section of S-bearing molecules after ion bombardment of CO:H_2S ice mixture at 20 K. In particular they have studied the destruction of H_2S and the formation of H_2S_2, OCS, SO_2, CS_2 and a S-rich residue. These values have been added to a chemical model to study the fate of S-bearing species in star forming regions.

5.4 Atom budget in chemical reactions

Neglecting projectile implantation, sputtering and nuclear reactions, the number of atoms for each element in a target under bombardment must remain constant. That is, what an ion beam does in a sample is to rearrange its atom positions, causing chemical reactions and structural changes. Infrared spectroscopy is a very suitable technique to monitor both modifications since the energies and intensities of photon absorption due to excitation of molecular vibration modes depend on local electrical dipoles, which in turn depend on the atom positions.

The connection between the infrared band absorbance, S, and the number of molecules per target area (column density, N) is given by the Lambert-Beer Law: $S = A\,N / (\ln 10)$. The quantity A, called the integrated absorption coefficient (A-value), is related to the oscillator strength of the transition. Besides being characteristic of molecular bonds, A is also a function of the sample temperature and of its crystallographic state, as well as of the chemical environment of the analyzed molecule. Due to the number of different experimental chemical environments, the value of A associated with a given transition of a certain molecule can vary; therefore, caution is necessary when cross sections obtained from distinct experiments are compared. To check if relative A-values are correct, the atom budget analysis is performed. It consists in determining the balance between the number of atoms missing in the precursor species and that detected in the daughter molecules. This procedure is done as a function of the beam fluence, and for each element existent in the sample, including the remaining initial molecules and the newly appearing molecules, as shown in Figure 9. In this comparison, it should be taken into account that not all the daughter species can be detected by FTIR.

The carbon budget of a H_2O:H_2CO:CH_3OH (100:2:0.8) ice mixture irradiated by 220 MeV $^{16}O^{7+}$ ions is illustrated in Figure 9 (data from de Barros *et al* 2014a). A very nice agreement between the total number of carbon atoms delivered by the H_2CO + CH_3OH precursors and the sum of carbon atoms attributed to the six formed molecular species is observed. An example of a triple element (hydrogen, carbon and oxygen) analysis on atom budget relative to the bombardment of a H_2O:CH_3OH ice mixture by 40 MeV Ni ions is presented in de Barros *et al* (2014b).

5.5. Ices containing mixtures of molecules: chemical complexity and organics

In space environments, although water ice often is the dominant component, other simple molecules are likely to be present, often in considerable fractions. In such mixtures of condensed "simple" molecules, after radiolysis the subsequently following chemical reactions become more complex and the spectrum of synthesized new molecular species becomes richer. There appears a trend towards chemical complexity possibly leading to the synthesis of organic and pre-biotic molecules if the main ingredients of organic chemistry (that is H, C, N and O) are present. Indeed, laboratory astrochemistry has shown that radiation processing of ices containing small molecules (H_2O, CO, CO_2, CH_3OH, NH_3, HCOOH) can lead to formation of complex, organic molecules. Amino acids and nucleobases can be formed under interstellar/circumstellar conditions by vacuum UV irradiation, electron and ion bombardment (Bernstein *et al* 2002, Munoz-Caro *et al* 2002, de Marcellus *et al* 2015, Danger *et al* 2013, Nuevo *et al* 2010, Holtom *et al* 2005).

After swift heavy ions processing of ammonia-containing ices made of mixtures of small molecules such as H_2O:NH_3 and H_2O:NH_3:CO, IR spectra exhibited lines of several new species including HNCO, N_2O, OCN^-, and NH_4^+. After a slow warm-up to room temperature, the IR spectra of the residues from irradiated H_2O:NH_3:CO ice showed five bands tentatively assigned to vibration modes of zwitterionic glycine, an amino acid, and possibly, another can be attributed to hexamethylenetetramine (HMT) (Pilling *et al* 2010a).

Martinez *et al* (2014) employed the PDMS technique for studying the radiolysis of the CO NH_3 ice. The dependence of the ion desorption yield on the sample temperature was investigated and the emission process of the desorbed ions discussed. NH_4^+, HCO^+, NO^+, NH_3OH^+, NH_3CO^+, CN^- and OCN^- secondary ions were observed after the projectile impact. From these measurements, it can be concluded that NH_4^+ and OCN^- ions are abundantly formed by the interaction of cosmic rays with CO−NH_3 ices.

Several studies have focused on the comparison between the effects induced by UV photolysis and ion irradiation of ice mixtures. Experimental results have shown that from a qualitative point of view, ion irradiation and UV photolysis generate similar changes in ice samples. However, quantitative differences between the two processes have been observed.

As an example, in studies of N_2 ices, Hudson and Moore (2002) discovered that while the N_3 (azide) radical was readily formed after bombardment with 0.8 MeV protons, photolysis by far-UV did not result in the detection of N_3. However, studies by Wu *et al* (2012) have shown that UV photolysis of thick (about 160 μm) solid N_2 samples does indeed produce N_3, suggesting that some N_3 was produced in the experiments of Hudson & Moore, albeit in very small quantities below their detection limit. Furthermore, Kobayashi *et al* (2007) irradiated gas mixtures of carbon monoxide, nitrogen, and water using UV light, soft X-rays, gamma-rays and particle beams of hydrogen (protons), helium, carbon, neon, and argon ions to investigate the production of complex organic species. They found that when N_2 molecules were used as the nitrogen source, amino acids precursors were not detected

after photolysis with UV light, but were detected after processing with the particle beams, gamma-rays, or X-rays. Kobayashi *et al.* ascribed this effect to the inability of UV light to dissociate either CO or N_2 molecules. Furthermore, in the case that ammonia was used, amino acid precursors were detected in all the cases, but the formation cross section by high energy particles was much higher than those by UV or X-ray photons.

A comparison between the formation of products in an ice mixture of interstellar type both by irradiation of the ice using swift heavy ions and by vacuum UV photons using a similar energy dose (in eV/molecule) was done by Munoz-Caro *et al* (2014). They demonstrated that irradiation processing of ices containing methanol and ammonia CH_3OH:NH_3 by both UV photons and swift heavy ions yield similar residues containing organic molecules after warm-up to room temperature of the irradiated ices. In order to confirm and quantify the possible formation of even more complex organic molecules, ex-situ chromatographic analysis of thick residues from swift ion processing is necessary.

Recently Islam *et al* (2014) have compared the effects of ion irradiation and UV photolysis on CH_3OH:N_2 ice mixture with the aim to investigate the effect of the occurrence of these two processes in tandem and separately. They found that when UV photolysis and ion bombardment act separately, their effects are very similar from a qualitative point of view, while significant quantitative difference may exist. In the case of simultaneous processing they did not detect any synergistic effect, but, in some instances the behavior of newly formed species (such as CH_4) can significantly depend on the UV/ions dose ratio.

These studies touch the question of the origin of organic matter on Earth: organics produced by irradiation of condensed molecules at low temperature could thus be present in circumstellar regions and comets, and were likely delivered to the primitive Earth bringing potential building blocks for the emergence of life on earth, and possibly on other bodies (not only?) in the Solar System (Ehrenfreund *et al* 2002). In this respect, other studies have focused on the formation of formamide after UV photolysis and ion irradiation of simple ices (e.g. Bernstein *et al* 1995; Demyk *et al* 1998; Gerakines *et al* 2004; Henderson and Gudipati 2015; Kaňuchová *et al* 2016). Formamide (NH_2HCO) is the simplest naturally occurring amide. This compound contains in its structure all the elements that are required for the synthesis of biomolecules, specifically, hydrogen, carbon, oxygen, and nitrogen, with the only exception of phosphorus and sulfur. Although formamide is easily formed by the reaction of hydrogen cyanide with water, it has been suggested that it can be directly delivered to Earth by comets and cometary debris.

Lv *et al* (2014) have studied NH_3:CO_2 and H_2O:NH_3:CO_2 ice mixtures at 16 K. They have found that upon warming up to 160 K, complex chemical reactions occur leading to the formation of new molecules and, in particular, ammonium carbamate and carbamic acid dimer. After UV photolysis or ion irradiation of the same ice samples new chemical species are formed such as ammonium formate, carbamic acid dimer, CO and OCN^- (e.g. Bossa *et al* 2008; Lv *et al* 2014). Both ammonium formate and carbamic acid are important species for prebiotic chemistry.

In recent years, ice mixtures containing molecular nitrogen have attracted particular interest, since nitrogen is common e.g. on TNO's and difficult to detect in IR studies (Boduch *et al* 2012). As an example, de Barros *et al* (2015) studied heavy ion induced radiolysis of ices made of 90% N_2 and 10% H_2O. The nitrogen oxides NO_3, NO_2 and N_2O are the most abundantly formed molecules. Therefore, the presence of nitrogen oxides may be a good indicator for the N_2 concentration in a TNO exposed to energetic particles. N_2O dominates with about 50% of the column density of the produced species and is the most likely chemical species expected to be detected on TNO surfaces dominated by N_2 in the presence of water. Indeed, only NO, N_2O, O_3 and HNO were detected so far in space environments.

Augé *et al* (2016) studied N_2-CH_4 ice mixtures with a dominating nitrogen content of up to 98%. Irradiation with swift heavy ions at 14 K led to formation of HCN and CN^-. During annealing of the irradiated ices (heating up to room temperature) a solid residue is formed containing poly-HCN like material, which may be a precursor of organic material observed in ultra-carbonaceous micrometeorites collected in Antarctica (UCAMMs). The infrared spectra of the solid residues measured at room temperature show indeed similarities with that of UCAMMs, and also with that of poly-HCN (Bonnet *et al* 2015). The associated formation time scales are compatible with radiation induced processing of icy bodies orbiting in the outer Solar System.

5.6 Radioresistance of complex organic molecules

Complex molecules can be formed under interstellar conditions by vacuum UV irradiation and also ion bombardment of ices at frozen surfaces in the Solar System such as comets, asteroids and in several moons of the giant planets (Ehrenfreud and Charnley 2000). Nucleobases were found in the Murchison meteorite (Martins *et al* 2000). The simplest amino acid, glycine (NH_2CH_2COOH), has been recently detected among the compounds collected by the space probe STARDUST around comet Wild 2 (Elsila, Galwin and Dworkin 2009). It is then also necessary and pertinent to study the radiation resistance (stability) of such complex molecules when exposed to radiation and to perform estimations of survival lifetimes (see also section 5.3).

Portugal *et al (*2014) have performed irradiation experiments on condensed glycine molecules with swift heavy ions showing the stability of glycine in a solid phase (crystalline α-glycine form) under ion bombardment. Very recently, the radiolysis of nucleobases under heavy ion impact was investigated. These nitrogen-containing biological compounds the basic building blocks of deoxyribonucleic acid (DNA) and ribonucleic acid (RNA). The primary nucleobases are cytosine (C), guanine (G), adenine (A), thymine (T) and uracil (U), of which A, G, C, and T appear in DNA and A, G, C, and U in RNA. Muniz *et al* (2016) reported that Adenine destruction cross sections, similar to what was observed with smaller molecules, follow a power law $\sim S_e^n$, with n = (1.17 ± 0.06) as a function of the electronic stopping power. As radiolysis products, newly arising IR absorption bands

can be attributed to HCN, CN^-, $C_2H_4N_4$, CH_3CN and $(CH_3)_3CNC$. The half lifetime of solid adenine exposed to cosmic rays was estimated as $(10\pm8) \times 10^6$ years.

6. Molecule formation after implantation

The surfaces of icy satellites of the giant planets are dominated by water ice layers that are much ticker than the penetration depth of the energetic magnetospheric particles (keV-MeV). Thus the incoming ions remain trapped in the target (implantation). If these ions are reactive (e.g., H^+, C^+, N^+, O^+, S^+) they induce all of the effects of any other ion but in addition have a chance to form new species containing the projectile. In the last two decades, numerous studies have been performed on the implantation of 1's-100's keV reactive ions in several icy mixtures. In Table 2 we present a list of the experimental results obtained so far. Such kinds of experiments are important to get insight into the debate on the origin of the minor molecular species that have been detected on the surface of the icy satellites.

Among the most recent implantation experiments there are those relative to multiply charged carbon and sulfur ions. Carbon implantation in pure water ice efficiently produces carbon dioxide. Nevertheless, it has been confirmed that, given the present estimate of the carbon ion fluxes in the Jovian magnetosphere, this cannot be the only source of the observed CO_2 on the Galilean satellites (Strazzulla *et al* 2003b; Lv *et al* 2012). An alternative suggested mechanism is based on the presence of refractory carbons (and/or organics) native or released by meteoritic impacts. Water could be deposited on those carbon-containing materials and form an ice/solid interface. Ion irradiation at the interface efficiently removes carbon from the solid and produces mainly carbon dioxide (Mennella *et al* 2004; Gomis and Strazzulla 2005; Raut *et al* 2012; Sabri *et al* 2015). Such a finding is relevant in the debate on the so-called "carbon cycle" in which the carbon-bearing species, i.e. amorphous carbon, carbonates and carbon chains, and CO_2 are continuously recycled. In fact, once formed, carbon dioxide results to be mixed with water ice (and other trace species), and it is then subjected to radiolysis as discussed above (section 5).

Studies of sulfur implantation in water ice were motivated by the search for the synthesis of SO_2 that could be produced by S^{n+} implantation (e.g. Hendrix *et al* 2011). Surprisingly, experiments have shown a very efficient synthesis of hydrated sulfuric acid after implantation of 50-200 keV S^{n+} (n=1-11) ions (Strazzulla *et al* 2007, Ding *et al* 2013). SO_2 is not detected after implantation in water ice, only an upper limit to the production yield of about 0.025 SO_2 molecules/ion has been obtained. Thus sulfur implantation is able to explain the synthesis of the hydrated sulfuric acid for which a strong correlation with the local flux of magnetospheric sulfur ions has been demonstrated (Dalton *et al* 2013).

However, SO_2 is observed after implantation of sulfur ions in frozen CO_2. Possibly, also CS_2 is produced (Lv *et al* 2014). This latter molecule has not yet been detected on icy satellites and should be searched for in future space missions. The formation of sulfur dioxide is interesting and points out towards a reciprocal influence of sulfur and carbon cycles. Although at present it is not possible to

draw definitive conclusions, it has been suggested that the observed SO_2 could be formed by sulfur ion implantation in ices dominated by water but containing carbon dioxide at the level of 1 % (Lv *et al* 2014).

7. Final remarks

A wealth of information has been obtained by laboratory experiments simulating radiation effects in ices by cosmic rays, not only with photons, electrons and protons, but also with heavier ionic projectiles. The latter have also been used to study chemistry induced by implantation. Most of the information was obtained by FTIR and TOF-SIMS spectroscopy. These techniques used to get information on the induced effects need to be improved and additional techniques could be developed as discussed e.g. in Allodi *et al* (2013). There are already attempts to use additional techniques, being many orders of magnitude more sensitive than those used so far, aimed at studying the effects induced by energetic processing of ices.

To name a few examples, a novel application of reflectron time-of-flight (ReTOF) mass spectrometry coupled to soft photoionisation has been developed at the University of Hawaii (Jones and Kaiser 2013) to probe the molecules formed upon interaction of ionising radiation (5 keV electrons) with simple ices on line and in situ. At the Leiden (Holland) Observatory a new ultra-high vacuum experiment is operative (Paardekooper *et al* 2014) that allows studying photo-induced chemical processes in interstellar ice analogues by combining laser desorption and time-of-flight mass spectrometry with the goal to characterize the solid state evolution of organic compounds upon UV photolysis. At JPL (USA) a two-color laser-desorption laser-ionisation time-of-flight mass spectroscopic method (2C-MALDI-TOF) has been developed and used to probe the effects of UV photons on polycyclic aromatic hydrocarbon (PAH) molecules embedded in water-ice at 5 K (Gudipati and Yang 2012).

Along similar lines, the installation of a new and innovative experimental set-up is in progress at INAF - Osservatorio Astrofisico di Catania (Italy); the aim is the detection of specific complex molecules formed on ice samples after bombardment with fast ions (100-400 keV) by using a combination of laser desorption, jet cooling, laser ionisation followed by high resolution time of flight mass-spectrometric analysis (Palumbo *et al* 2016). At CIMAP in Caen, a new irradiation set-up equipped with FTIR and UV-visible spectrometers was built. The IGLIAS setup is an ultrahigh vacuum chamber equipped with a cold head. It will provide the possibility to prepare samples of simple or mixed ices (up to four components) under highly improved ultrahigh vacuum conditions. It is mounted on a mobile support and can thus be installed at different beamlines at GANIL (from keV/u to MeV/u projectile energy). After a commissioning phase, it will be opened to use by the scientific community, access being granted by the interdisciplinary program advisory committee at GANIL.

CIMAP's TOF-SIMS set-up (Allodi *et al* 2013, Hijazi *et al* 2011, Martinez *et al* 2015) has been equipped with a cold head allowing to condense gases on a Cu surface and to prepare thin ice samples. First results concern the contribution of clusters ejected from water ice during sputtering by slow highly charged ions. An upgrade with a Quartz-Crystal Microbalance (QCM) to study thin film growth, sublimation, and desorption (Allodi *et al* 2013) will be used to control the thickness of the deposited ice. Also, experiments with biomolecules covered by a water layer (or in a water matrix) can be envisaged. With the TOF technique, it will be possible to detect the fragments of the mother biomolecule and to understand the direct destruction mechanisms of the biomolecules and their radioresistance. In this respect, the radiation induced chemistry at interfaces of carbon containing materials (PAH, complex biomolecules) and ices come into mind. The possibility of combining SIMS and beam focusing techniques, like electromagnetically focused ion beams FIB, which are already widely applied (Nan Yao 2007) or possibly in the near future, nano-beams obtained by guiding in glass capillaries, may allow spatially resolved analysis of inhomogeneous surfaces and spatially resolved implantation.

Finally, it might be interesting to study realistic radiation fields, with different particles affecting the ices simultaneously. Possibly, synergy effects may be observed in a laboratory simulation of a complex irradiation field with photons, electrons, and ions. In this vein, it is also interesting to remind that surfaces in space may be simultaneously processed by radiation and micrometeorite impact.

Acknowledgements

This work was supported by the Italian Ministero dell'Istruzione, dell' Università e della Ricerca through the grant Progetti Premiali 2012-iALMA (CUP C52I13000140001), by the Italian Space Agency (ASI 2013-056 JUICE Partecipazione Italiana alla fase A/B1), PHC Capes-Cofecub France-Brésil, the Brazilian Agencies CNPq and FAPERJ, the EU Cost Action "The Chemical Cosmos", the Chinese Scholarship Council CSC, la Région Basse Normandie, the SPIRIT (EU) and EMIR (France) networks, the European Commission FP7 for RTD Capacities Program (Contract No. 262010 ENSAR), the French INSU-CNRS program Physique et Chimie du Milieu Interstellaire (PCMI) and the ANR IGLIAS, grant ANR-13-BS05-0004 of the French Agence Nationale de la Recherche. It is a pleasure to thank our colleagues from CIMAP and GANIL for their invaluable support. Special thanks also to all of our co-authors.

References

Allodi M A *et al* 2013 *Space Sci. Rev.* **180** 101-175

Andrade D P P, Rocco M L M., Boechat-Roberty H M, Iza P, Martinez R, Homem M G P and da Silveira E F 2007 *J. Electron. Spectrosc. Relat. Phenom.* **155** 124-8

Andrade D P P, Boechat-Roberty H M, Martinez R, Homem M G P, da Silveira E F and Rocco M L M 2009 *Surf. Sci.* **603** 1190-6

Andrade D P P, de Barros A L F, Pilling S, Domaracka A, Rothard H, Boduch P and da Silveira E F 2013 *Mon. Not. R. Astron. Soc.* **430** 787-96

Andrade D P P, de Barros A L F, Ding J J, Rothard H, Boduch P and da Silveira E F 2014 *Mon. Not. R. Astron. Soc.* **444** 3792 -801

Augé B, Dartois E, Engrand C, Duprat J, Godard M, Delauche L, Bardin N, Mejía C, Martinez R, Muniz G, Domaracka A, Boduch P and Rothard H 2016 *Astron. Astrophys.* **592** A99

Aumayr F and Winter H P 2004 *Phil. Trans. R. Soc.* A **362** 77-102

Assmann W, Toulemonde M and Trautmann C 2007 Total sputtering yield of materials irradiated in the electronic energy loss regime in *Topics in Applied Physics* vol **110** (Behrisch R and Eckstein W) pp 403-93

Barth C A, Hord C W, Stewart A I F, Pryor W R, Simmons K E, McClintock W E, Ajello J M, Naviaux K L and Aiello J J 1997 *Geophys. Res. Lett.* **24** 2147-2150

Bahr D A, Famà M, Vidal R A and Baragiola R A 2001 *J. Geophys. Res.* **106** 33285-90

Baragiola R A, Vidal R A, Svendsen W, Schou J, Shi M, Bahr D A and Atteberrry CL *Nucl. Instr. Meth. Phys. Res.* B **209** 294-303

Baratta G A, Arena M M, Strazzulla G, Colangeli L, Mennella V and Bussoletti E 1996 *Nucl. Instr. Meth. Phys. Res.* B **116** 195-9

Baratta, G. A, Leto G, Spinella F, Strazzulla G and Foti G 1991 *Astron. Astrophys.* **252** 421-4

Baratta G A, Leto G and Palumbo M E 2002 *Astron. Astrophys.* **384** 343-9

Baratta G A, Domingo M, Ferini G, Leto G, Palumbo ME, Satorre M A and Strazzulla G 2003 *Nucl. Instr. Meth. Phys. Res.* B **209** 283-7

Baratta G A, Chaput D, Cottin H, Fernandez Cascales L, Palumbo M E and Strazzulla G 2015 *Planet. Space Sci.* **118** 211-20

Bar-Nun A, Herman G, Rappaport M L and Mekler Y 1985 *Surf. Sci.* **150** 143-56

Barros Leite C V, da Silveira E F, Jeronymo J M F, Pinho R R, Baptista G B, Schweikert E A and Park M A 1992 *Phys. Rev.* B **45** 12218-21

Behrisch R and Eckstein W (eds) 2007 *Sputtering by Particle Bombardment: Experiments and Computer Calculations from Threshold to MeV Energies* (Springer Verlag, Berlin, New York, Heidelberg)

Benit J, Bibring, J-P and Rocard F 1988 *Nucl. Instr. Meth. Phys. Res.* B 32, 349-53

Bennett C J, Pirim C and Orlando T M 2013 *Chem. Rev.* **113** 9086-150

Benninghoven A 1969 *Physica Status Solidi* **34** K169-K171

Betts L, da Silveira E F and Schweikert E A 1995 *Int. J. Mass Spectrom.* **145** 9-23

Bergantini A, Pilling S, Rothard H, Boduch P and Andrade D P P 2014 *Mon. Not. R. Astron. Soc.* **437** 2720–7

Bernstein M P, Sandford S A, Allamandola L J, Chang S and Scharberg M A 1995 *Astrophys. J.* **454** 327-44

Bernstein M P, Dworkin J P, Sandford S A, Cooper G W and Allamandola L J 2002 *Nature* **416** 401-3

Bethe H 1932 *Zs. f. Phys.* **76** 293-9

Bethe H 1930 *Ann. d. Phys.* **5** 325-400

Betz H D 1972 Rev. *Mod. Phys.* **44** 465-539

Bloch F 1933a *Zs. f. Phys.* **81** 363-76

Bloch F 1933b *Ann. d. Phys.* **16** 285-320

Boduch P, Domaracka A, Fulvio D, Langlinay T, Lv XY, Palumbo M E, Rothard H and Strazzulla G 2012 *Astron. Astrophys.* **544** A30

Boduch P, da Silveira E F, Domaracka A, Gomis O, Lv X Y, Palumbo M E, Pilling S, Rothard H, Duarte E S and Strazzulla G 2011 *Advances in Astronomy* Article ID 327641

Boduch P *et al* 2015 *J. Phys. Conf. Series* **629** 012008

Bohr N 1948 *Kgl. Danske Vidensk. Selsk. Mat. Fys. Medd.* XVIII No. 8

Bonnet J-Y *et al* 2015 *Icarus* **250** 53-63
Boogert A C, Gerakines P A and Whittet D C B 2015 *Ann. Rev. Astron. Astrophys.* **53** 541-81
Bordalo V, da Silveira E F, Lv X Y, Domaracka A, Rothard H, Seperuelo Duarte E and Boduch P 2013 *Astrophys. J.* **774** 105
Bossa J B, Theulé P, Duvernay F, Borget F and Chiavassa T 2008 *Astron. Astrophys.* **492** 719-24
E.M. Bringa and R.E. Johnson 2003 Ion interactions with solids: astrophysical applications *Solid State Astrochemistry* ed Pirronello V, Krelowski J and Manicò G (Kluwer Academic Publishers) pp 357-93
Brown I G (ed) 2004 The Physics and Technology of Ion Sources, 2nd, Revised and Extended Edition (Wiley-VCH)
Brown L W, Augustyniak M W, Marcantonio K J, Simmons E H, Boring J W, Johnson R E and Reimann C T 1984 *Nucl. Instr. Meth. Phys. Res.* B **1** 307-14
Brucato J R, Palumbo M E and Strazzulla G 1997 Icarus **125** 135-44
Brunetto R, Loeffler M J, Nesvorný D, Sasaki S and Strazzulla G 2015 Asteroid surface alteration by space weathering processes *Asteroids IV* ed Michel P, Demeo F E, and Bottke W F (University of Arizona Press, Tucson) pp 597–616
Buch V and Devlin J P 1991 *J . Chem. Phys.* 94 4091-92.
Busch K L and Cooks R G 1982 *Science* **218** 247-54
Capaccioni F *et al* 2015 *Science* **347** aaa0628 (23 Jan 2015)
Carlson R W, Johnson R E and Anderson M S 1999 Science **286** 97-9
Carlson R W, Anderson M S, Johnson R E, Schulman M B and Yavrouian, A H 2002 *Icarus* **157** 456-63
Cassidy T A, Johnson R E and Tucker O J 2009 *Icarus* **201** 182-90
Chabot M 2016 *Astron. Astrophys.* **585** A15
Chrisey D B, Brown W L and Boring J W1990 *Surf. Sci.* **225** 130-42
Chyba C F 2000 *Nature* **403** 381-382
Collado V M, Farenzena L S, Ponciano C R, da Silveira E F and Wien K 2004 *Surf. Sci.* **569** 149- 62
Compagnini G, D'Urso L, Puglisi O, Baratta G A and Strazzulla G 2009 *Carbon* **47** 1605-7
Constantini J-M, Couvreur F, Salvetat J-P and Bouffard S 2002 *Nucl. Instr. Meth. Phys. Res.* B **194** 132- 40
Cooper J F, Johnson R E, Mauk B H, Garrett H B and Gehrels N 2001 *Icarus* **149** 133-59
Cooper J F, Christian E R, Richardson J D and Wang C 2003 *Earth, Moon and Planets* **92** 261–77
Dalton J B, Cruikshank D P, Stephan K, McCord T B, Coustenis A, Carlson R W and Coradini A 2010 *Space Science Reviews* **153** 113
Dalton J B, Cassidy T, Paranicas C, Shirley J H, Prockter L M and Kamp L W *Planet. Space Sci.* **77** 45-63
Danger G, Orthous-Daunay F-R, de Marcellus P, Modica P, Vuitton V, Duvernay F, Le Sergeant d'Hendecourt L, Thissen R. and Chiavassa T 2013 *Geochimica & Cosmochimica Acta* 184-201
Dartois E *et al* 1998 *Astron. Astrophys.* **338** L21-4
Dartois E *et al* 2013a *Astron. Astrophys.* **557** A97
Dartois E *et al* 2013b *Icarus* **224** 243-52
Dartois E *et al* 2015a *Astron. Astrophys.* **576** A125
Dartois E *et al* 2015b *Nucl. Instr. Meth. Phys. Res.* B **365** 472-6
de Barros A L F, Bordalo V, Seperuelo Duarte E, da Silveira E F, Domaracka A, Rothard H and Boduch 2011a *Astron. Astrophys.* **531** A160
de Barros A L F, Domaracka A, Andrade D P P, Boduch P, Rothard H and da Silveira E F 2011b *Mon. Not. R. Astron. Soc.* **418** 1363–74
de Barros A L F, Farenzena L S, Andrade D P P, da Silveira E F and Wien K 2011c *J. Phys. Chem.* **115** 12005-14
de Barros A L F, da Silveira E F, Pilling S, Domaracka A, Rothard H and Boduch P 2014a *Mon. Not. R. Astron. Soc.* **438** 2026–35
de Barros A L F, da Silveira E F, Rothard H, Langlinay T and Boduch P 2014b *Mon. Not. R. Astron. Soc.* **443** 2733-45
de Barros AL F, da Silveira E F, Bergantini A, Rothard H and Boduch P 2015 *Astrophys. J.* **810** 156

de Barros AL F, da Silveira E F, Fulvio D, Rothard H and Boduch P 2016 *Astrophys. J.* **824** 81
Della Negra S, Jacquet D, Lorthiois I, Lebeyec Y, Becker O and Wien K 1983 *Int. J. Mass. Spectrom.* **53** 215-26
de Marcellus P, Meinert C., Myrgorodska I, Nahon L, Buhse T, Le Sergeantd'Hendecourt L and Meierhenrich U J 2015 *Proc. Natl. Acad. Sci.* **112** 965-70
Demyk K, Dartois E, d'Hendecourt L, Jourdain de Muizon M, Heras A M and Breitfellner M 1998 *Astron. Astrophys.* **339** 553-60
Ding J J, Boduch, P Domaracka A, Guillous S, Langlinay T, Lv X Y, Palumbo M E, Rothard H and Strazzulla G 2013 *Icarus* **226** 860-4
Draine B T 1978 *Astrophys. J. Supp. Series* **36** 595-619
Dukes C A, Chang W Y, Famá M and Baragiola R A 2011 *Icarus* **212** 463-9
Duprat J, Engrand C, Maurette M, Kurat G, Gounelle M and Hammer C 2007 *Adv. Space Res.* **39** 605-11
Echenique P M, Flores F and Ritchie R H 1990 *Solid State Phys.* **43** 229-308
Ehrenfreund P *et al* 2002 *Rep. Prog. Phys.* **65** 1427-1487
Ehrenfreund P and Charnley S B 2000 *Ann. Rev. Astron Astrophys.* **38** 427-83
Elsila J E, Glavin D P and Dworkin J P 2009 *Meteor. Planet. Sci.* **44** 1323–30
Ellegaard O, Schou J, Stenum B, Sorensen H, Pedrys R, Warczak B, Oostra D J, Haring E and de Vries A E 1994 *Surf. Sci.* **302** 371-84
Elman B S, Dresselhaus M S, Dresselhaus G, Maby E W and Mazurek H 1981 *Phys. Rev.* B **24** 1027
Elmegreen B G 2007 *Astrophys. J.* **668** 1064-82
Fama M, Loeffler M J, Raut U and Baragiola R A 2010 *Icarus* **207** 314-19
Farenzena L S *et al* 2005a *Earth, Moon, and Planets* **97** 311-29
Farenzena L S, Collado V M, Ponciano C R, da Silveira E F and Wien K 2005b *Int. J. Mass Spectrom.* **243** 85-93
Farenzena L S, Martinez R, Iza P, Ponciano C R, Homem M G P, Naves de Brito A, da Silveira E F and Wien K 200 *Int. J. Mass Spectrom.* **251** 1-9
Fernández-Lima F A, Ponciano C R, Faraudo G S, Grivet M, da Silveira E F and Chaer Nascimento M A 2007 *Chem. Phys.* **340** 127-33
Firsov O B 1959 *Sov Phys JETP* **36** 1076
Fitzpatrick E L and Massa D 2007 *Astrophys. J.* **663** 320
Fleischer R L, Price P B and Walker R M 1965 *J. Appl. Phys.* **36** 3645-52
Gaffey M J 2010 *Icarus* **209** 564-74
Garozzo M, Fulvio D, Gomis O, Palumbo M E and Strazzulla G 2008 *Planet Space Sci.* **56** 1300-08
Garozzo M, Fulvio D, Kanuchova Z, Palumbo M E and Strazzulla G 2010 *Astron. Astrophys.* **509** A67
Gavilan L, Alata I, Le K C, Pino T, Giuliani A and Dartois E 2016 *Astron. Astrophys.* **586** A106
Gerakines P A, Moore M H and Hudson R. L 2000 *Astron. Astrophys.* **357** 793-800
Gerakines P A., Moore M H and Hudson R L 2004 *Icarus* **170** 202-13
Gibb E L, Whittet D C B, Boogert A C A and Tielens A G G M 2004 *Astrophys. J. Supplement Series* **151** 35-73
Gomis O, Satorre M A, Strazzulla G and Leto G 2004 *Planet Space Sci.* **52** 371-8
Gomis O and Strazzulla G 2005 *Icarus* **177** 570-6
Gredel R, Lepp S, Dalgarno A and Herbst E 1989 *Astrophys. J.* **347** 289-93
Grundy W M, Buie M W, Stansberry J A, Spencer R J and Schmitt B 1999 *Icarus* **142** 536-49
Gudipati M S and Yang R 2012 *Astrophys. J. Lett.***756** L24
Hansen G B and McCord T B *2004 Proc. J. Geophys. Res.* **109** E01012
Hansen K C, Ridley A, Hospodarsky G B, Achilleos N, Dougherty M K, Gombosi T I, Tóth G 2005 *Geophys. Res. Lett.* **32** L20S06
Henderson B L and Gudipati M S 2015 *Astrophys. J.* **800** 66
Hendrix A R, Barth C A and Hord C W 1999 *J. Geophys. Res.* **104** 14169-78
Hendrix A R, Cassidy T A, Johnson R E, Paranicas C and Carlson R W 2011 *Icarus* **212** 736-43
Hendrix A R, Domingue D L and Noll K S 2013 Ultraviolet Properties of Planetary Ices *The Science of Solar System Ices* (ed) Gudipati M S and Castillo-Rogez J **356** pp 73-105
Hibbitts C A, Klemaszewski J E, McCord T B, Hansen G B and Greeley R 2002 *J. Geophys. Res. Planet.* **107** Id. 5084

Hibbitts C A, Pappalardo R T, Hanse G B and McCord TB 2003 *J. Geophys. Res. Planet.* **108** Id. 5036
Hijazi H *et al* 2011 *Nucl. Instr. Meth. Phys. Res.* B **269** 1003-6
Hilf E R, Tuszynski W, Curdes B, Curdes J, Wagner M and Wien K 1993 *Int. J. Mass Spectrom.* **126** 101-14
Holtom P D, Bennett C J, Osamura Y, Mason N J and Kaiser R I 2005 *Astrophys. J* **626** 940-52
Hudson R L and Moore M H1999 *Icarus* **140** 451-61
Hudson R L and Moore M H 2000 *Icarus* **145** 661-3
Hudson R L and Moore M H 2002 *Astrophys. J.* **568** 1095-99
Hudson R L, Moore M H and Cook A M 2005 *Adv. Space Res.* **36** 184-9
Islam F, Baratta G A, Palumbo M E 2014 *Astron. Astrophys.* **561** A73
Iza P, Farenzena L S and da Silveira E F 2007 *Nucl. Instr. Meth. Phys. Res.* B **5** 483-8
Jackson J D 1975 *Classical Electrodynamics* John Wiley&Sons (New York)
Johnson R E, Cooper J F, Lanzerotti L J and Strazzulla G 1987 *Astron. Astrophys.* **187** 889-92
Johnson R E *1990 Energetic Charged-Particle Interactions with Atmospheres and Surfaces* Springer-Verlag (Berlin, Heidelberg, New York)
Johnson R E, Carlson R W, Cooper J F, Paranicas C, Moore M H and Wong M C 2004 *Jupiter: Planet, Satellites, and Magnetosphere* ed. by Bagenal F, McKinnon W and Dowling T (Cambridge Univ. Press, Cambridge, UK,) pp 485-512
Johnson R E, Pospieszalska M and Brown W L 1991 *Phys. Rev.* B **44** 7263-72
Johnson R E and Schou J 1993 Sputtering of Inorganic Insulators in *Fundamental Processes in the Sputtering of Atoms and Molecules* (ed. P. Sigmund) *Mat. Fys. Medd.* **43** pp 403-93
Jones B M and Kaiser R I 2013 *J. Phys. Chem. Lett.* **4** 1965-71
Jones B M, Kaiser R I and Strazzulla G 2014a *Astrophys. J.* **781** Id. 85
Jones B M, Kaiser R I and Strazzulla G 2014b *Astrophys. J.* **788** Id. 170
Kalish R, Reznik A, Nugent K W and Prawer S 1999 *Nucl. Instr. Meth. Phys. Res.* B **148** 626-33
Kalvans J 2015 *Astron. Astrophys.* **573** A38
Kaňuchová Z, Brunetto R, Melita M and Strazzulla G 2012 *Icarus* **221** 12-9
Kaňuchová Z, Urso R G, Baratta G A, Brucato J R, Palumbo M E and Strazzulla G 2016 *Astron. Astrophys.* **585** A155
Kessler M F *et al* 1996 *Astron. Astrophys.***315** L27-31
Kobayashi K *et al* 2007 *IEEJ Transactions on Electronics, Information and Systems* **127** 293-8
Léger A., Jura M and Omont A 1985 *Astron. Astrophys.* **144** 147-60
Leto G and Baratta G A 2003 *Astron. Astrophys.* **397** 7-13
Lindhard J 1954 *Kgl. Danske Vidensk. Selsk. Mat. Fys. Medd.* **XXVIII** No. 8
Lindhard J, Scharff M and Schiøtt H E 1963 *Kgl. Danske Vidensk. Selsk. Mat. Fys. Medd.* **XXXIII** No. 14
Loeffler M J, Baratta G A, Palumbo M E, Strazzulla G and Baragiola R A 2005 *Astron. Astrophys.* **435** 587-94
Loeffler M J, Raut U, Vidal R A, Baragiola R A and Carlson R W 2006 *Icarus* **180** 265-73
Loeffler M J, Hudson R L, Moore M H and Carlson RW 2011 *Icarus* **215** 370-80
Loeffler M J and Hudson R L 2012 *Icarus* **219** 561-6
Lv X Y*et al* 2012 *Astron. Astrophys.* **546** A81
Lv X Y, Boduch P, Ding J J, Domaracka A, Langlinay T, Palumbo M E, Rothard H and Strazzulla G 2014 *Mon. Not. R. Astron. Soc.* **438** 922-9
Lv X Y, Boduch P, Ding J J, Domaracka A, Langlinay T, Palumbo M E, Rothard H and Strazzulla G 2014 *Phys. Chem. Chem. Phys.* **16** 3433-41
Maldoni M M, Egan M P, Smith R G, Robinson G and Wright C M 2003 *Mon. Not. R. Astron. Soc.* **345** 912-22
Macfarlane R D and Torgerson D F 1976 *Int. J. Mass Spectrom.* **21** 81-92
Martinez R, Ponciano C R, Farenzena L S, Iza P, Homem M G P, Naves de Brito A, da Silveira E F and Wien K *Int. J. Mass Spectrom.* **252** (2007a) 195-202
Martinez R, Farenzena LS, Iza P, Ponciano C R, Homem M G, de Brito A N, Wien K and da Silveira EF *Int. J. Mass Spectrom.* **42** (2007b) 1333-41
Martinez R, Bordalo V, da Silveira E F and Boechat-Roberty H M 2014 *Mon. Not. R. Astron. Soc.* **444** 3317-27
Martinez R, Langlinay T, Boduch P, Cassimi A, Hijazi H, Ropars R, Salou P, da Silveira E F and

Rothard H 2015 *Mater. Res. Express* **2** 076403
Martins Z, Botta O, Fogel M L, Sephton M A, Glavin D P, Watson J S, Dworkin J P, Schwartz AW, Ehrenfreund P 2008 *Earth Planet. Sci. Lett.* **270** 130-6
Mejía C F, de Barros A L F, Bordalo V, da Silveira E F, Boduch P, Domaracka A and Rothard H 2013 *Mon. Not. R. Astron. Soc.* **433** 2368–79
Mejía C F, de Barros A L F, Seperuelo Duarte E, da Silveira E F, Dartois E, Domaracka A, Rothard H and Boduch P 2015a *Icarus* **250** 222 – 9
Mejía C F, Bender M, Severin D, Trautmann C, Boduch P, Bordalo V, Domaracka A, Lv X Y, Martinez R and Rothard H 2015b *Nucl. Instr. Meth. Phys. Res.* B **365** 477-81
Mennella V, Palumbo M E and Baratta G A 2004 *Astron. Astrophys.* **615** 1073-80
Modica P and Palumbo M E 2010 *Astron. Astrophys.* **519** A22
Molinari S, Ceccarelli C, White G J, Saraceno P, Nisini B, Giannini T and Cauxet E1999 *Astrophys. J. Lett.* **521** L71
Moore M H and Hudson R L 1992 *Astrophys. J.* 401, 353-60
Moore M H and Hudson R L 2000 *Icarus* **145** 282-8
Moore M H and Khanna R K 1991 *Spectrochimica Acta Part* A **47** 255-62
Moore M H and Hudson R L 2003 *Icarus* **161** 486-500
Moore M H, Hudson R L and Carlson R W 2007 *Icarus* **189** 409-23
Moore M H, Ferrante R F, Hudson R L and Stone J N 2007 *Icarus* **190** 260-73
Muñoz Caro G M, Meierhenrich U J, Schutte W A, Barbier B, Arcones Segovia A, Rosenbauer H, Thiemann W H-P, Brack A and Greenberg J M 2002 *Nature* 416 403-6
Muñoz Caro G M, Dartois E, Boduch P, Rothard H, Domaracka A and Jiménez-Escobar A 2014 *Astron. Astrophys.* **566** A93
Murakami *et al* 2007 *Publications of the Astronomical Society of* Japan **59** S369
Mouschovias T C, Tassis K and Kunz M W 2006 *Astrophys. J.* **646** 1043-9
Neugebauer G *et al* 1984 *Astrophys. J. Lett.* **278** L1-6
Nuevo M, Bredehöft J H, Meierhenrich U J, d'Hendecourt L andThiemann W H-P 2010 *Astrobiology* **10** 245-56
Occhiogrosso A, Viti S, Modica P and Palumbo M E 2011 *Mon. Not. R. Astron. Soc.* **418** 1923
Öberg K I, Fuchs G W, Awad Z, Fraser H J, Schlemmer S, van Dishoeck E F and Linnartz H 2007 *Astrophys. J. Lett.* 662 L23
Öberg K I, Bottinelli S, Jørgensen J K and van Dishoeck E F 2010 *Astrophys. J.* **716** 825-34
Öberg K I, Boogert A C A, Pontoppidan K M and Van den Broek S 2011 *Astrophys. J.* **740** 109
Omont A, Forveille T, Moseley S H, Glaccum W J, Harvey P M, Likkel L, Loewenstein R F and Lisse C M 1990 *Astrophys. J. Lett.* **355** L27-30
Ottaviano L, Palumbo M E and Strazzulla G 2000 *Conf. Proc. SIF* **68** p 149
Paardekooper D M, Bossa J-B, Isokoski K and Linnartz H 2014 *Rev. Sci. Instrum.* **85** 104501
Padovani M, Hennebelle P and Galli D 2013 *Astron. Astrophys.* **560** A114
Palumbo M E 1997*Adv.Space Res.* **20** 1637-48
Palumbo M E 2006 *Astron. Astrophys.* **453** 903-9
Palumbo M E, Leto P, Siringo C and Trigilio C 2008 *Astrophys. J.* **685** 1033-8
Palumbo M E, Baratta G A, Leto G and Strazzulla G 2010 *J. Mol. Structure* **972** 64-7
Palumbo ME, Urso R G, Kanuchova Z, Scirè C, Accolla M, Baratta G A and Strazzulla G 2016 *EAS Publications Series* in press
Peeters Z, Hudson R L, Moore M H and Lewis A. 2010 *Icarus* **210** 480-7
Pilling S, Seperuelo Duarte E, da Silveira E F, Balanzat E, Rothard H, Domaracka A and Boduch P 2010a *Astron. Astrophys.* **509** A87
Pilling S, Seperuelo Duarte E, Domaracka a, Rothard H, Boduch p and da Silveira E F 2010b *Astron. Astrophys.* **523** A77
Pilling S, Andrade D P P, da Silveira E F, Rothard H, Domaracka A and Boduch P 2012 *Mon. Not. R. Astron. Soc.* **423** 2209-21
Plainaki C, Milillo A, Mura A, Orsini S, Massetti S and Cassidy T 2012 *Icarus* **218** 956-66
Plainaki C, Milillo A, Mura A, Saur J, Orsini S and Massetti S 2013 *Planet. Space Sci.* **88** 42-52
Ponciano C R, Farenzena L S, Collado V M, da Silveira E F and Wien K 2005 *Int. J. Mass Spectrom.* 244 41-9

Ponciano C R, Martinez R, Farenzena L S, Iza P, da Silveira E F, Homem M G P, Naves de Brito A and Wien K 2006 *J. Am. Soc. Mass Spectrom.* **17** 1120-8
Ponciano C R, Martinez R, Farenzena L S, Iza P, Homem M G P, Naves de Brito A, Wien K and da Silveira E F 2008 *J. Mass Spectrom.* **43** 1521-30
Portugal W, Pilling S, Boduch P, Rothard P and Andrade D P P 2014 *Mon. Not. R. Astron. Soc.* **441** 3209–25
Puglisi O, Compagnini G, D'Urso L, Baratta G A, Palumbo M E and Strazzulla G 2014 *Nucl. Instr. Meth. Phys. Res.* B **326** 2-6
Raut U, Teolis B D, Loeffler M J, Vidal R A, Fam M and Baragiola R A 2007 *J. Chem. Phys.* **126** 244511-15
Raut U, Fulvio D, Loeffler M J and Baragiola R A 2012 *Astrophys. J.* **752** Id. 159
Rothard H and Gervais B 2006 Electron emission from solids irradiated with swift ion beams in *Ion Beam Science - Solved and Unsolved Problems* (ed P Sigmund) *Mat. Fys. Medd.* **52** pp 497-524
Sabri T, Baratta G A, Jger C, Palumbo M E, Henning T, Strazzulla G and Wendler E 2015 *Astron. Astrophys.* **575** A76
Sack N J, Boring J W, Johnson R E, Baragiola R A and Shi M 1991 *J. Geophys. Res.* **96** l7535-40
Seitz F and Koehler J S 1956 Displacement of atoms during irradiation in *Solid State Physics* ed Seitz F and Turnbull D Vol. **2** (Academic Press, New York) pp 308-48
Seperuelo Duarte E, Boduch P, Rothard H, Been T, Dartois E, Farenzena L S and da Silveira E F 2009 *Astron. Astrophys.***502** 599-603
Seperuelo Duarte E, Domaracka A, Boduch P, Rothard H, Dartois E and da Silveira E F 2010 *Astron. Astrophys.***512** A71
Sessler A and Wilson E (ed) 2007 *Engines of Discovery - A Century of Particle Accelerators* World Scientific Publishing Co. Pte. Ltd. (Singapore)
Shemansky D E, Yung Y L, Liu X, Yoshii J, Hansen C J, Hendrix A R and Esposito L *Astrophys. J.* **797** 84
Shematovich V I, Johnson R E, Cooper J F , Wong M C 2005 *Icarus* **173** 480-98
Sigmund P 1969 *Phys. Rev.* **184** 383-416
Sigmund P (ed) 1993 Fundamental Processes in Sputtering of Atoms and Molecules *K. Dan. Vid. Selsk. Mat. Fys. Medd.* **43**
Sigmund P 2006 Particle penetration and radiation effects. General Aspects and Stopping of Swift Point Charges *Springer Series in Solid State Sciences* **151**
Sigmund P 2014 Particle penetration and radiation effects. Volume 2: Penetration of Atomic and Molecular Ions *Springer Series in Solid State Sciences* **179**
Smyth W H and Marconi M L 2006 *Icarus* **181** 510-26
Spohr R (ed) 1990 *Ion Tracks and Microtechnology - Principles and Applications*Vieweg (Braunschweig)
Stephens W E 1946 *Phys. Rev.* **69** 691-3
Strazzulla G 1999 *Planet. Space Sci.* **47** 1371-6
Strazzulla G 2011 *Nucl. Instrum. Meth. Phys. Res. B* **269** 842–51
Strazzulla, G and Johnson R E 1991 in: *Comets in the post- Halley Era* (eds.) Newburn Jr. R L, Neugebauer M and Rahe J Kluwer Publ. Co. (London) pp 243-276
Strazzulla G, Baratta G A, Johnson R E and Donn B 1991 *Icarus* **91** 101-4
Strazzulla G and Baratta G A 1992 *Astron. Astrophys.* **266** 434-8
Strazzulla G, Baratta G A and Palumbo M E 2001 Spectrochimica Acta **57** 825-842
Strazzulla G, Cooper J F, Christian E R and Johnson R E 2003a *Comptes Rendus Physique* **4** 791-801
Strazzulla G, Leto G, Gomis O and Satorre M A2003b *Icarus* **164** 163-9
Strazzulla G, Leto G, Spinella F and Gomis O 2005*Astrobiology* **5** 612-21
Strazzulla G, Baratta A, Leto G and Gomis O 2007 *Icarus* **192** 623-8
Sundqvist B U R 1992 *Int. J. Mass Spectrom.* **118/119** 265-87
Schiwietz G and Grande P L 2011 *Phys. Rev. A* **84** 052703
Teolis B D, Loeffler M J, Raut U. Famà M and Baragiola R A 2006 *Astrophys. J.* **644** L141-4
Wagner M, Wien K, Curdes B and Hilf E R 1993 *Nucl. Instrum. and Meth.* B **82** 362-78
Waite J H *et al* 2009 Nature **460** 487-90
Werner M W *et al* 2004 *Astrophys. J. Supp. Series* **154** 1-9

Wien K, Becker O, Guthier W, Matthäus R and Moshammer R 1991 *Int. J. Rad.App. Instrum.* D **19** 971–4
Woods P M, Occhiogrosso A, Viti S, Kanuchova Z, Palumbo M E and Price S D *Mon. Not. R. Astron. Soc.* **450** 1256-67
Wu Y-J, Wu C Y R, Chou S-L, Lin M-Y, Lu H-C and Cheng B-M 2012 *Astrophys. J* **746** 175-86
Wille K 2001 *The Physics of Particle Accelerators- An Introduction* (translated by McFall J) Clarendon Press (Oxford University Press)
Vignoli Muniz G S, Mejia C F, Martinez R, Auge B, Rothard H, Domaracka A and Boduch P 2016 *Astrobiology* submitted
Yao N (ed) 2007 *Focused Ion Beam Systems, Basics and Applications* (Cambridge University Press)
Zheng W and Kaiser R I 2007 *Chem. Phys. Lett.* **450** 55-60
Ziegler J F, Biersack J P and Ziegler M D 2008*The Stopping and Range of Ions in Matter* ISBN 0-9654207-1-X http://www.srim.org/

TARGET	PROJECTILE	G-Value (molecules /100 eV)	Daughter Molecules	References
CO	50 MeV Ni^{13+}	-5.9	CO_2, O_3, C_3O_2, C_5O2, C_2O, C_3	Seperuelo et al. 2010
	537 MeV Ni^{24+}	-2.5		
	0.2 MeV H^+	-0.79		Loeffler et al. 2005
CH_4	220 MeV O^{7+}	-4.97	CH_3, C_2H_2, C_2H_4, C_2H_6, C_3H_8	de Barros et al. 2011a
CH_3OH	774 MeV Kr^{31+}	-190	H_2CO, CH_2OH, CH_4, CO, CO_2 ,	de Barros et al. 2011b
	606 MeV Zn^{26+}	-70	HCO, $HCOOCH_3$	
	16 MeV O^{5+}	-7.9		
	220 MeV O^{7+}	-0.76		
CH_3COCH_3	40 MeV Ni^{11+}	-0.69 (*)	CH_4, CO,H_2CO, CO_2, C_2H_4, C_2H_6	Andrade et al. 2014
c-C_6H_{12}	220 MeV O^{7+}	-2.9	CH_4, Alkenes	Pilling et al. 2012
NH_3	537 MeV Ni^{24+}	-4.3	H_2, N_2, N_2H_2, N_2H_4	Bordalo et al. 2013

Table 1 Radiochemical yields *G (*molecules/100eV*)* for the destruction of initial molecules obtained with initially pure ices taken from the given references. Formation of the indicated daughter molecules is discussed in those references. (*) calculated from the cross section given in the paper.

ION (E in keV)	TARGET T= 10-150 K	MAJOR PRODUCED SPECIES (In bold those containing the projectile)	References
H (1.5, 30-100)	CO_2	CO, $\mathbf{H_2CO_3}$, CO_3, O_3 $\mathbf{O-H}$ in poly-water	Brucato et al. 1997
	SO_2	SO_3, polySO_3, O_3, elemental S	Garozzo, et al 2008
C^{n+} (10, 30) n=1-3	H_2O	H_2O_2, $\mathbf{CO_2}$	Strazzulla, et al. 2003b Lv et al. 2012
	H_2O:N_2:O_2	$\mathbf{CO_2}$, $\mathbf{CO}$, NO, NO_2, N_2O, O_3	Boduch, et al. 2012
	N_2:O_2	$\mathbf{CO_2}$, $\mathbf{CO}$, NO, NO_2, N_2O, O_3	Boduch, et al. 2012
N (15, 30)	H_2O	H_2O_2	Strazzulla, et al. 2003b
	H_2O;CH_4	C_2H_6, CO, CO_2, $\mathbf{OCN^-}$, $\mathbf{HCN}$	Strazzulla 1999
O (30)	CH_4	C_2H_6, C_2H_4	Palumbo 1997
	N_2:CH_4	C_2H_6, C_2H_4, HCN	Ottaviano et al. 2000
S^{n+} (35-200) n=1-11	H_2O	H_2O_2, hydrated $\mathbf{H_2SO_4}$	Strazzulla et al. 2007 Ding et al. 2013
	CO	CO_2, $\mathbf{SO_2}$, $\mathbf{OCS}$?	Lv et al. 2014
	CO_2	CO, $\mathbf{SO_2}$, $\mathbf{CS_2}$?	Lv et al. 2014

Table 2 Summary of reactive ion implantation experiments. The major produced species that contain the projectile are indicated in bold face in column 3.

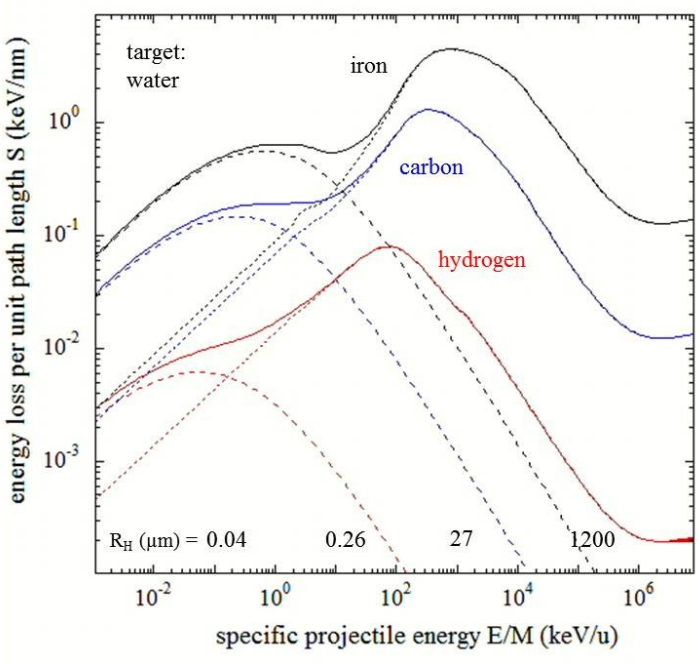

Figure 1. Total (full line), nuclear (dashed line) and electronic (dotted line) stopping power calculated with the SRIM software (Ziegler, Biersack and Ziegler 2008) for hydrogen, carbon and iron projectiles in water. The ranges (maximum implantation depth) R_H (measured in microns) for hydrogen projectiles of 100 eV, 10 keV, 1 MeV and 100 MeV are indicated.

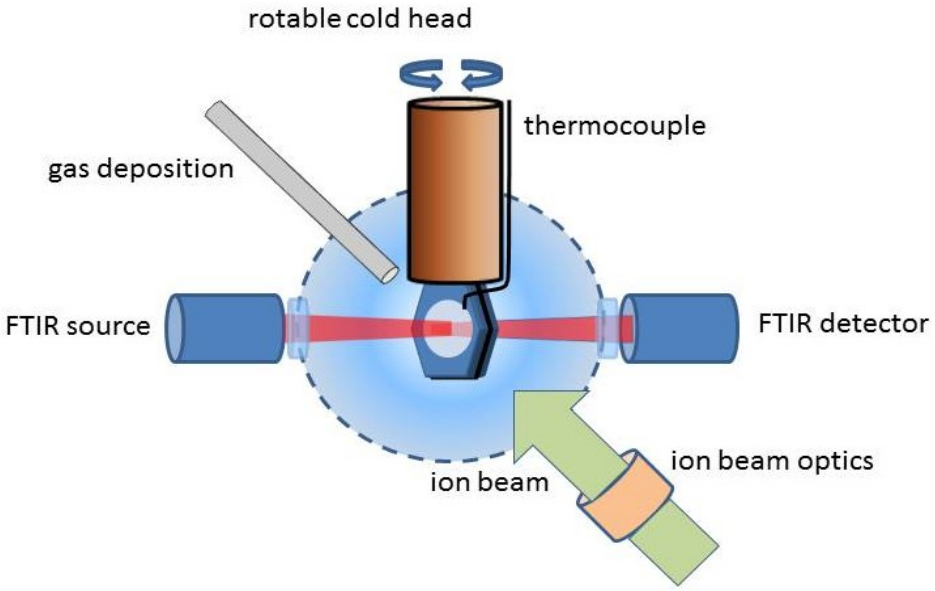

Figure 2. Schematic drawing of an irradiation set-up for ices by ion beams at low temperatures. The projectiles impinge on a thin sample prepared on a cold IR transparent window, which is analysed (in this example) by Fourier Transform Infrared absorption spectroscopy FTIR.

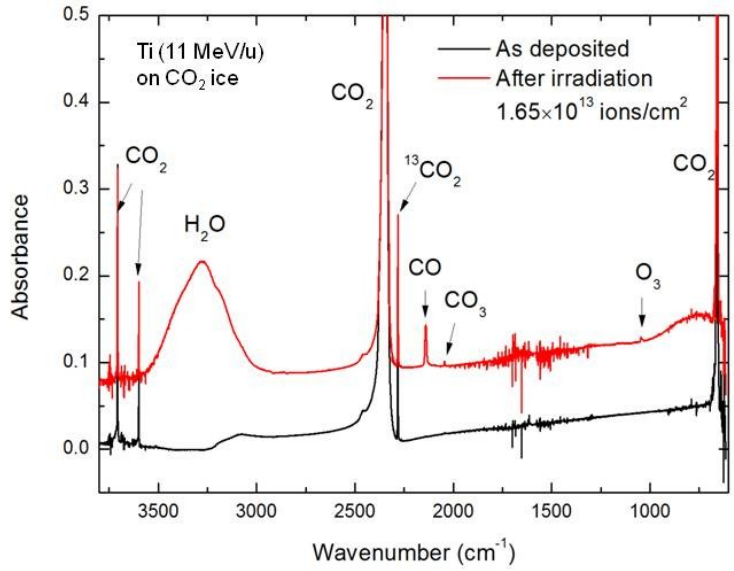

Figure 3. FTIR spectra of CO_2 ice, unirradiated (as deposited) and after irradiation with $^{50}Ti^{21+}$ ions of 11.4 MeV/u at a projectile fluence of 1.65×10^{13} ions cm^{-2}. Data are from the measurement campaign reported in Mejia *et al* 2015b.

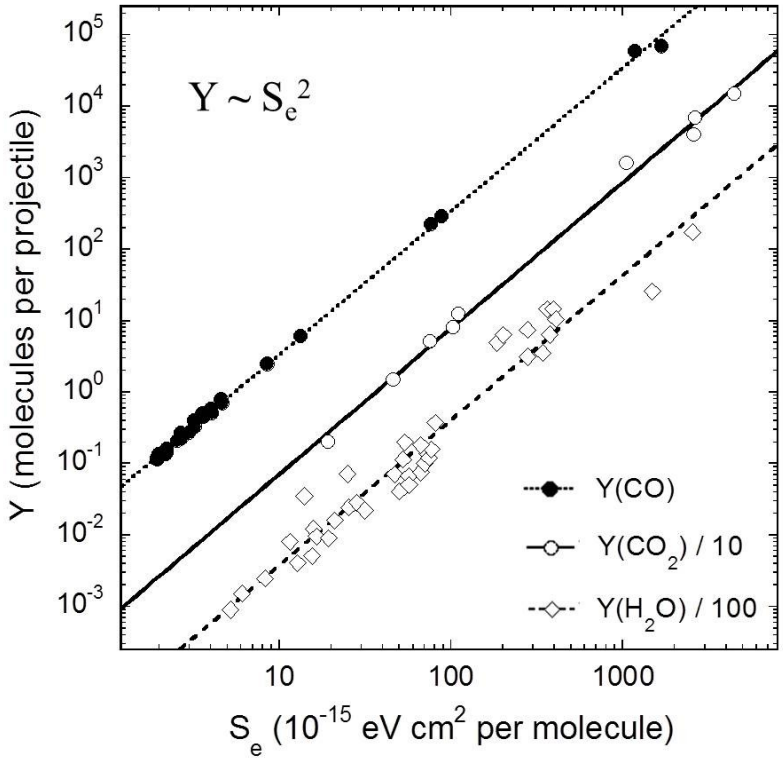

Figure 4. Sputtering yields as a function of the electronic stopping power S_e. Adapted from Boduch *et al* (2015), Mejía *et al* (2015b) and Dartois *et al* (2015a) for CO, CO_2 and H_2O, respectively. The

electronic stopping power S_e was calculated with the SRIM software (Ziegler, Biersack and Ziegler 2008). For clarity, the yield values for CO_2 were divided by 10 and those of H_2O by 100.

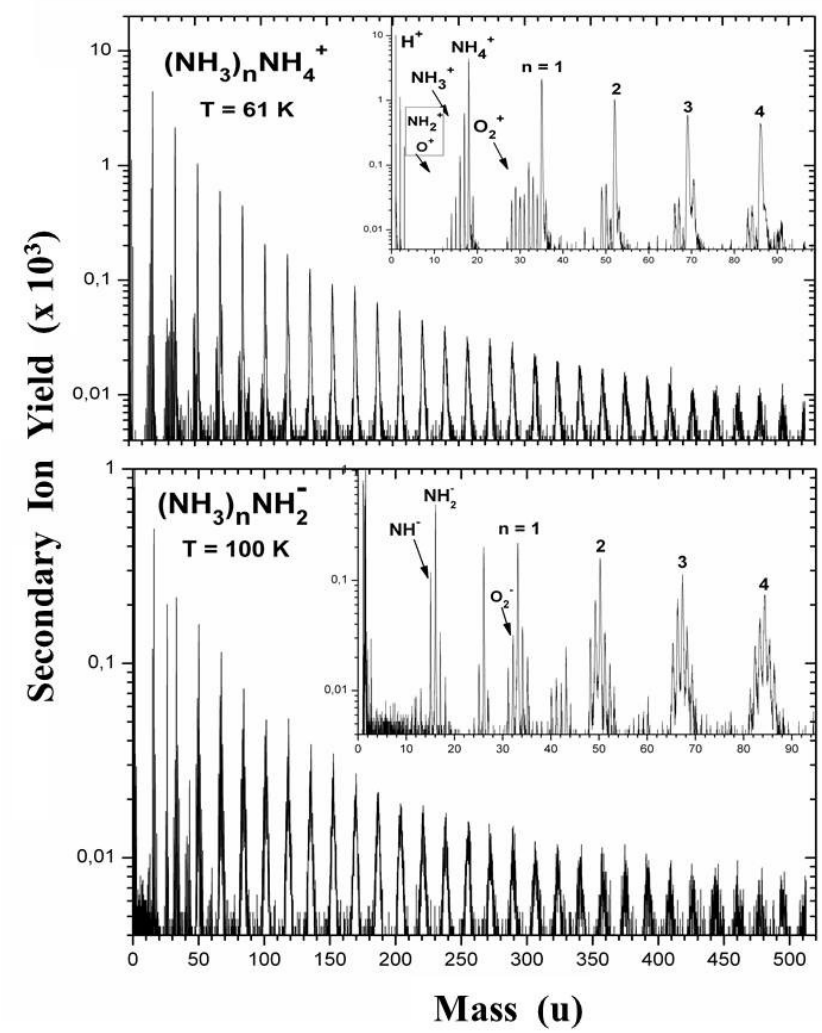

Figure 5. TOF-SIMS spectra of positive (top) and negative (bottom) secondary ions from NH_3 ice obtained by PDMS. The insets show the lower mass range up to 100 u. Adapted from Farenzena *et al* (2005a).

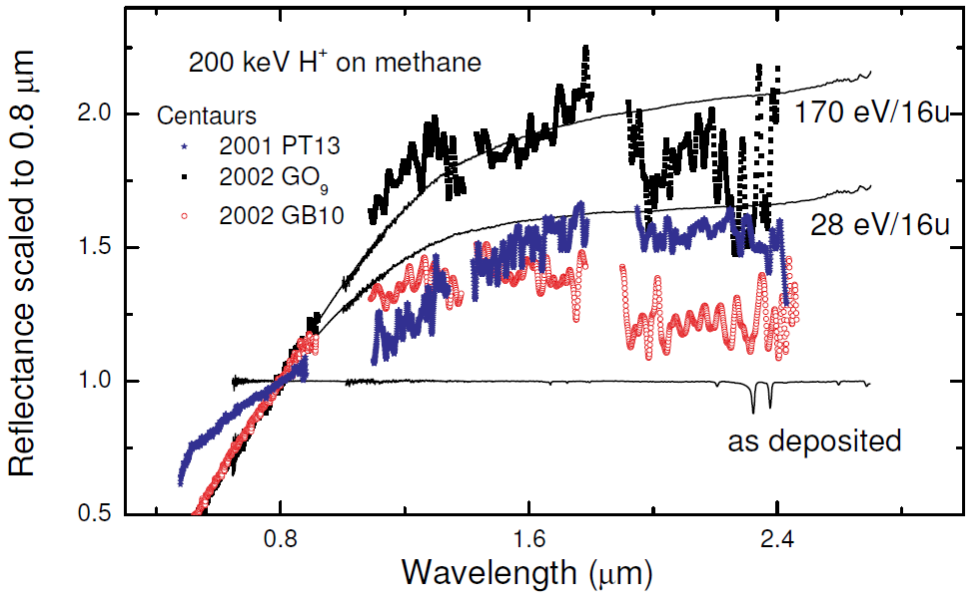

Figure 6. Reflectance spectra, scaled to 1 at 0.8 μm, of (16 K) methane as deposited and after irradiation with 200 keV H^+ ions at two different doses. The spectra of three Centaurus objects exhibiting different colors (spectral slopes) are also shown.

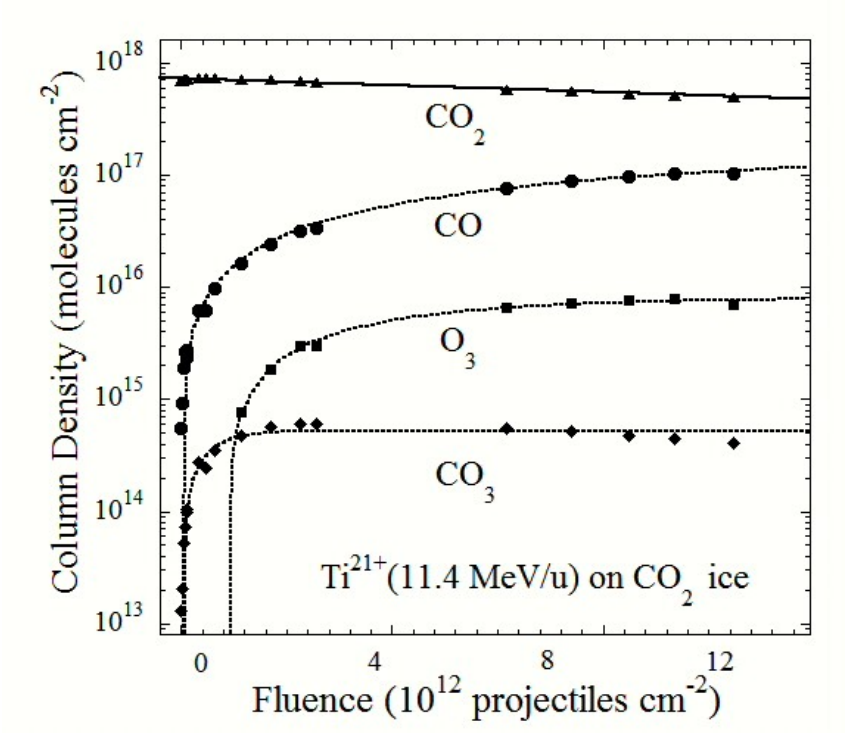

Figure 7. Column densities ("thickness") of CO_2 (top) and of the newly appearing molecules CO, CO_3, and O_3 (bottom, as indicated) as a function of projectile fluence during irradiation with $^{50}Ti^{21+}$ ions of 11.4 MeV/u (adapted from Mejia *et al* 2015b).

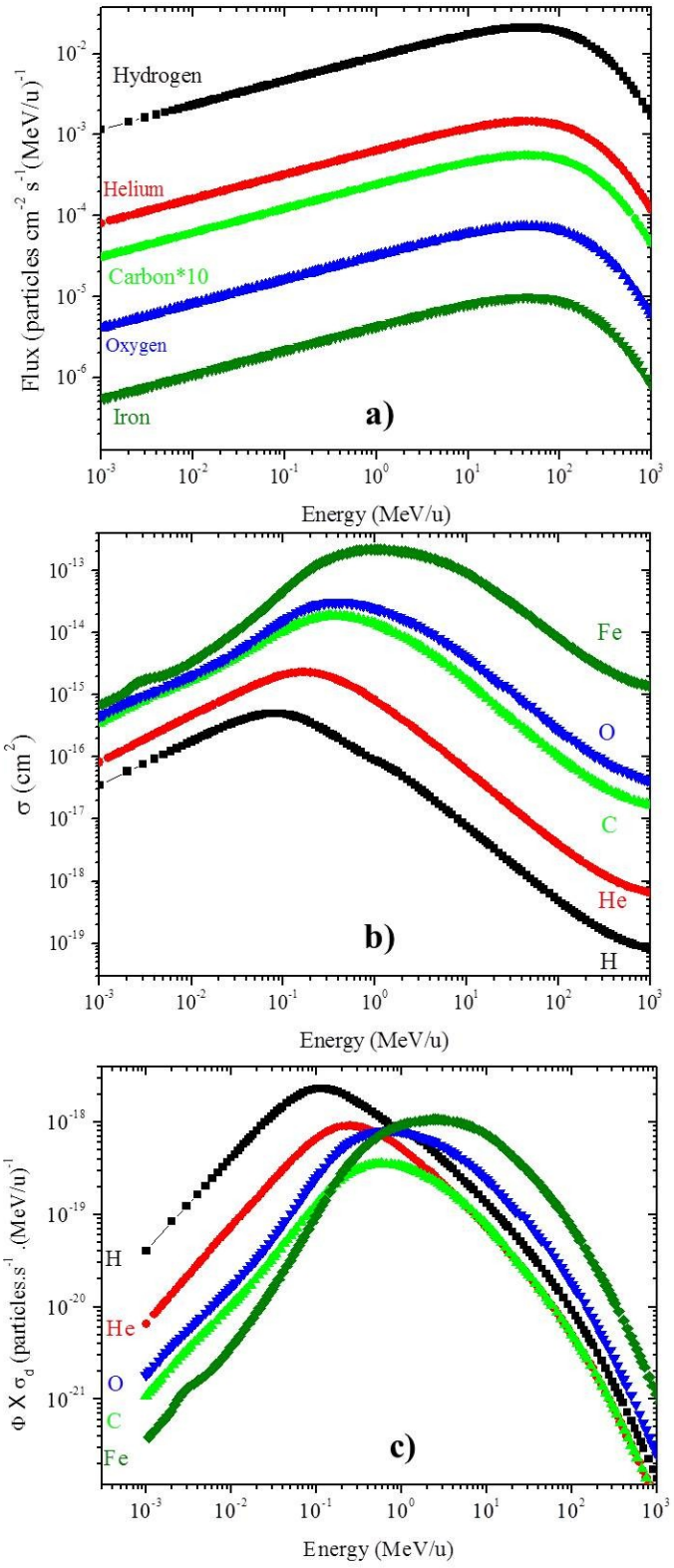

Figure 8. Ion flux in the ISM (a), predicted cross section (b) and dissociation rate (cross section times particle flux) (c) of frozen formic acid as a function of projectile energy. Projectiles shown are H, He, C, O and Fe. Adapted from Andrade *et al* (2013). Note in (c) that, for E > 10 MeV/u, the destruction rate due to Fe ion bombardment is greater than that due to the other projectile species.

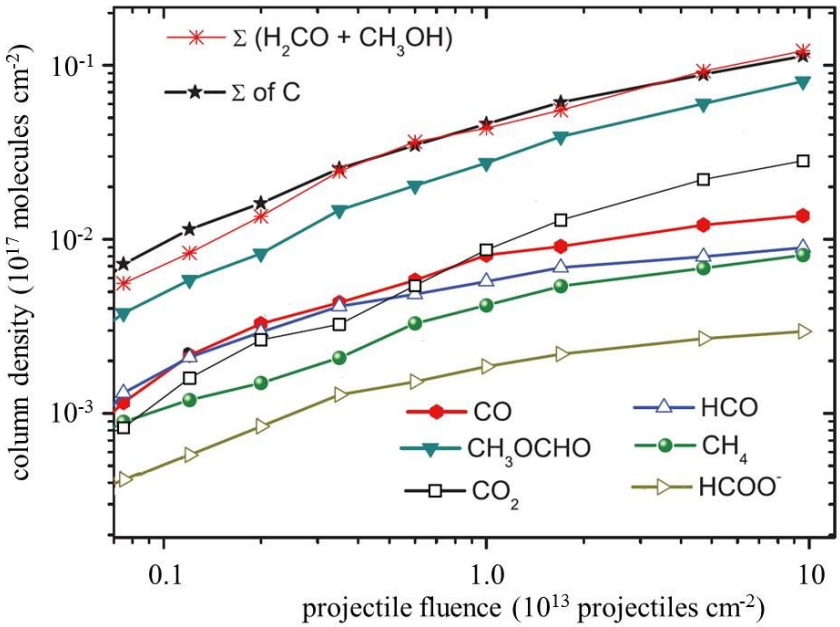

Figure 9. The total and partial carbon column densities of a H_2O:H_2CO:CH_3OH (100:2:0.8) ice mixture irradiated by 220 MeV $^{16}O^{7+}$ ions as a function of projectile fluence. The partial values were determined according to the carbon stoichiometry (data taken from de Barros et al 2014a).